# Accepted Manuscript


CureCuma–cationic curcuminoids with improved properties and enhanced antimicrobial photodynamic activity

Andreas Spaeth, Andre Graeler, Tim Maisch, Kristjan Plaetzer

PII: S0223-5234(17)30787-0

DOI: 10.1016/j.ejmech.2017.09.072

Reference: EJMECH 9787

To appear in: *European Journal of Medicinal Chemistry*

Received Date: 25 February 2017

Revised Date: 20 June 2017

Accepted Date: 29 September 2017

Please cite this article as: A. Spaeth, A. Graeler, T. Maisch, K. Plaetzer, CureCuma–cationic curcuminoids with improved properties and enhanced antimicrobial photodynamic activity, *European Journal of Medicinal Chemistry* (2017), doi: 10.1016/j.ejmech.2017.09.072.

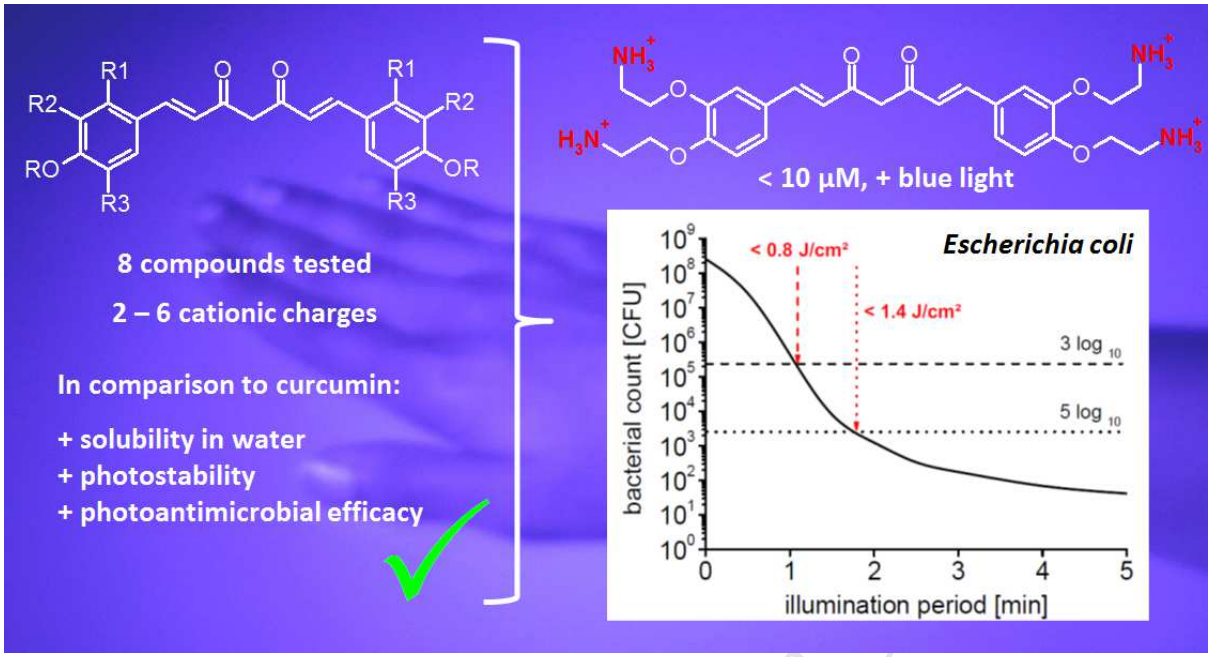

# CureCuma – Cationic curcuminoids with improved properties and enhanced antimicrobial photodynamic activity

Andreas Spaeth[1*], Andre Graeler[2], Tim Maisch[3] and Kristjan Plaetzer[2]

1 Department of Organic Chemistry, University of Regensburg, Regensburg, Germany

2 Laboratory of Photodynamic Inactivation of Microorganisms, Department Cell Biology and Physiology, University of Salzburg, Salzburg, Austria

3 Department of Dermatology, University Medical Centre Regensburg, Regensburg, Germany

*** Corresponding author:**

Andreas Späth, PhD

Department of Organic Chemistry

University of Regensburg

Universitätsstraße 31, 93040 Regensburg, Germany

e-mail: andreas.spaeth@chemie.uni-regensburg.de

Tel.: +49 941 943 4087

## Keywords

antimicrobial

photodynamic

curcumin

diferoylmethane

cationic photosensitizer

*Escherichia coli*

## Abstract

The naturally occurring photosensitizer curcumin has excellent biocompatibility, but its antimicrobial photodynamic efficacy is limited by (i) weak adherence to Gram(-) cell walls, (ii) low (photo-)stability and (iii) limited solubility in water.

In this study novel curcuminoids bearing cationic substituents were prepared by different synthetic routes. The derivatives exhibit excellent water solubility, improved photostability and low aggregation.

All novel curcuminoids showed antibacterial photodynamic effects (>3 $\log_{10}$ reduction of CFU) against *Escherichia coli* and *Staphylococcus aureus* upon blue light illumination. In contrast to natural curcumin, effective photokilling of *E. coli* was possible without the addition of permeabilizing agents. Ten micromolar of the most active compound (**8**) achieved a 7 $\log_{10}$ decrease of *E. coli* after light activation with a fluence of 33.8 J/cm², whereas *S. aureus* was inactivated by more than 4 $\log_{10}$ at a fluence of 5.3 J/cm². Overall the reduction in bacterial count was at least 100-fold more effective with these new curcuminoids in comparison to natural curcumin.

## Introduction

Humans are constantly exposed to pathogenic microorganisms and in most situations the immune system of healthy persons can handle bacterial attacks efficiently. In the past bacterial infections were easily cured by administration of antibiotics, but it is estimated that due to increasing antimicrobial resistance 10 million lives a year and a cumulative 100 trillion USD of economic output are at risk by 2050.[1] The extensive use and also misuse of antibiotics in human and veterinary medicine poses a huge selection pressure towards resistance.[2] It facilitates the fast spread of genes encoding antibiotic resistance within a bacteria population, providing a competitive advantage of such mutated resistant strains. As a consequence resistance to antibiotics is dramatically increasing. The development of new antibiotics is not able to keep up with the evolutionary pace. Only two new classes of antibiotics (oxazolidinone, cyclic lipopeptide) have been marketed in the past 15 years, which are active against Gram(+) bacteria, such as MRSA (*methicillin-resistant Staphylococcus aureus*). For Gram(-) bacteria the situation is even more critical.[3]

The WHO addresses antibiotic resistance as one of the most urgent priorities for public health and stated that this “a problem so serious that it threatens the achievements of modern medicine”[4] and the CDC report of 2013 calls the development of antibioitic resistance “one of our most serious health threats “.[5] In the recent UN General assembly it was stated that antibiotic resistant bacteria will render high-quality universal healthcare coverage more difficult if not impossible and undermine sustainable food production.[6]

This situation not only demands new antibiotics urgently, but also development of alternative disinfection approaches, which do not initiate resistance. In addition, adjuvants to conventional antibiotics, like drug efflux pump inhibitors,[7] can be used to inhibit resistance or to potentiate the activity of antibiotics.[8] Alternative therapy or precaution treatments

include cold atmospheric pressure plasma,[9] monoclonal antibodies,[10] and phage treatment.[11]

Photodynamic inactivation of bacteria (PDI) could serve both, the medical and the food sector: a *per se* harmless photoactive compound, the photosensitizer (PS), is administered and subsequently excited by visible light of appropriate wavelengths to generate reactive oxygen species (ROS). Photocatalytical ROS formation occurs via effective intersystem crossing and in consequence charge transfer to generate radicals (Type I photochemical reaction) or energy transfer to produce singlet oxygen (Type II photochemical reaction). The short-lived ROS immediately attack cellular structures and biomolecules in close proximity. The irreversible damage to the pathogens is caused by multi-target processes, thus avoiding rapid development of resistances of the microorganisms.[12] PDI has proven highly efficient against fungal, viral or bacterial infections.[13] In case that application of such light-activated PS are designated for food decontamination, decolonization of livestock or treatment of infection, the photosensitizer molecule should feature high biocompatibility, a negligible toxicity profile, accessibility for a reasonable price, and good biodegradability yielding only non-toxic fragments. In this regard, natural molecules, like curcumin /curcuma, with photosensing abilities should be considered.

Curcuma, obtained from the dried and grounded rhizome of *Curcuma longa* and *Curcuma domestica*, has been used for centuries as spice, in medicine, cosmetics and in fabric dying[14] and is attributed to have anti-inflammatory and digestive properties.[15, 16]

The main ingredient of the plant extract is curcumin (1,7-bis(4-hydroxy-3-methoxyphenyl)-1,6-heptadiene-3,5-dione), a diferuloylmethane with bright orange color. Intensive research over the last decades showed its high therapeutic and pharmacological potential[17, 18]: Several studies confirm anti-inflammatory[19], anti-rheumatic,[20, 21] anti-tumor[22, 23] and anti-carcinogenic[24] properties. Recently, the substance was discussed as therapeutic for Alzheimer´s disease.[25] These properties are mainly attributed to the antioxidant effects [17,

26] based on the elimination of free radicals [27, 28] and thereby reducing oxidative stress in the cell.[29, 30] There is also evidence that curcuminoids have antibacterial properties without illumination[31], but in presence of blue light curcumin shows clear phototoxic characteristics.[32]

Hydrogen bonding and charge delocalisation are important features of the molecule[33] for interactions with the outer bacterial cell wall,[34] and photochemical processes.[15] Nevertheless, its antimicrobial photodynamic efficacy is limited due to the weak adherence to Gram(-) bacteria,[12, 35, 36] but also due to low photostability and limited solubility of the natural substance. Limited photostability of a photosensitizer is not necessarily a major drawback of a photosensitizer, as it prevents long or pronounced photosensitivity after systemic administration. On the contrary, for disinfection high photostability provides a long-lasting antimicrobial effect.[37]

For the application of curcuminoids in clinical therapy and food preservation their photostability should be improved when compared to the natural compound, but not result in an extensive long-term stability. Derivatives should also feature lower anti-oxidative potential than curcumin for not counteracting photodynamic efficacy, but this property should not be entirely lost to maintain the health benefits of the natural molecule. Anti-oxidative properties of curcumin were mainly attributed to phenolic OH groups.[38, 39] Blocking these groups may result in lower pH sensitivity and as the central unit is not affected, the non-toxic nature of the chromophore should be maintained.

Addition of cationic charges has already been proven to enhance photodynamic effectivity against Gram(-) bacteria in other photosensitizer molecules like methylene blue.[40] In this study alkyl chains bearing cationic charged moieties are attached to the phenolic hydroxyl groups to the parent compound. Both the number of charges and the lipophilicity were altered in these derivatives, thereby enhancing the photodynamic inactivation efficacy.[40].

Therefore here we examine the impact of our approach of adding cationic charges to curcumin on photodynamic efficacy against two Gram(+) and Gram(-) bacterial model species (*S. aureus* and *E. coli*).

## Material and methods

### Characterization of prepared compounds

Thin layer chromatography (TLC) analyses were performed on silica gel 60 F-254 with 0.2 mm layer thickness and detection via UV light at 254 nm / 366 nm or through staining with ninhydrin in ethanol. Flash column chromatography was performed on Merck silica gel (Si 60 40-63 μm) either manually or on a Biotage® solera™ flash purification system. Column chromatography was performed on silica gel (70–230 mesh) from Merck.

Melting points were measured on a SRS melting point apparatus (MPA100 Opti Melt) and are uncorrected.

NMR spectra were recorded on Bruker Avance 300 ($^{1}$H 300.13 MHz, $^{13}$C 75.47 MHz, T = 300 K) or Bruker Avance 400 ($^{1}$H 400.13 MHz, $^{13}$C 100.61 MHz, T = 300 K) instruments. The chemical shifts are reported in δ[ppm] relative to external standards (solvent residual peak). The spectra were analyzed by first order, the coupling constants *J* are given in Hertz [Hz]. Characterization of the signals: s = singlet, d = doublet, t = triplet, q = quartet, m = multiplet, bs = broad singlet, psq = pseudo quintet, dd = double doublet, dt = doublet of triplets, ddd = double double doublet. Integration is determined as the relative number of atoms. Assignment of signals in $^{13}$C-spectra was determined with DEPT technique (pulse angle: 135 °) and given as (+) for $CH_3$ or CH, (–) for $CH_2$ and ($C_q$) for quaternary $C_q$. Error of reported values: chemical shift 0.01 ppm ($^{1}$H NMR) and 0.1 ppm ($^{13}$C NMR), coupling constant *J* 0.1 Hz. The solvents used for the measurements are reported for each spectrum.

IR spectra were recorded with a Bio-Rad FT-IR-FTS 155 spectrometer. Absorption spectra were recorded on a “Cary BIO 50” UV/VIS/NIR spectrometer from Varian. All measurements were performed in 1 cm quartz cuvettes (Hellma) and UV-grade solvents (Baker or Merck) at 25 °C.

Mass spectra were recorded on Finnigan MAT95 (EI-, CI- and FAB-MS), Agilent Q-TOF 6540 UHD (ESI-MS, APCI-MS) or Thermo Quest Finnigan TSQ 7000 (ES-MS, APCI-MS) spectrometer. Xenon serves as the ionization gas for FAB.

**Synthesis and purification of the compounds**

Commercial reagents and starting materials were purchased from Acros Organics, TCI Europe, Fluka, Merck or Sigma-Aldrich and used without further purification. The dry solvents tetrahydrofurane and dichloromethane were purchased from Sigma-Aldrich (puriss., absolute) or Roth (RotiDry Sept), respectively. They were stored over molecular sieves under nitrogen and were used as received. Curcumin (95 % purity) was purchased from ABCR and was purified by recrystallization from ethanol.

The PS presented in this study are water-soluble dyes based on the curcumin structure (**1**).

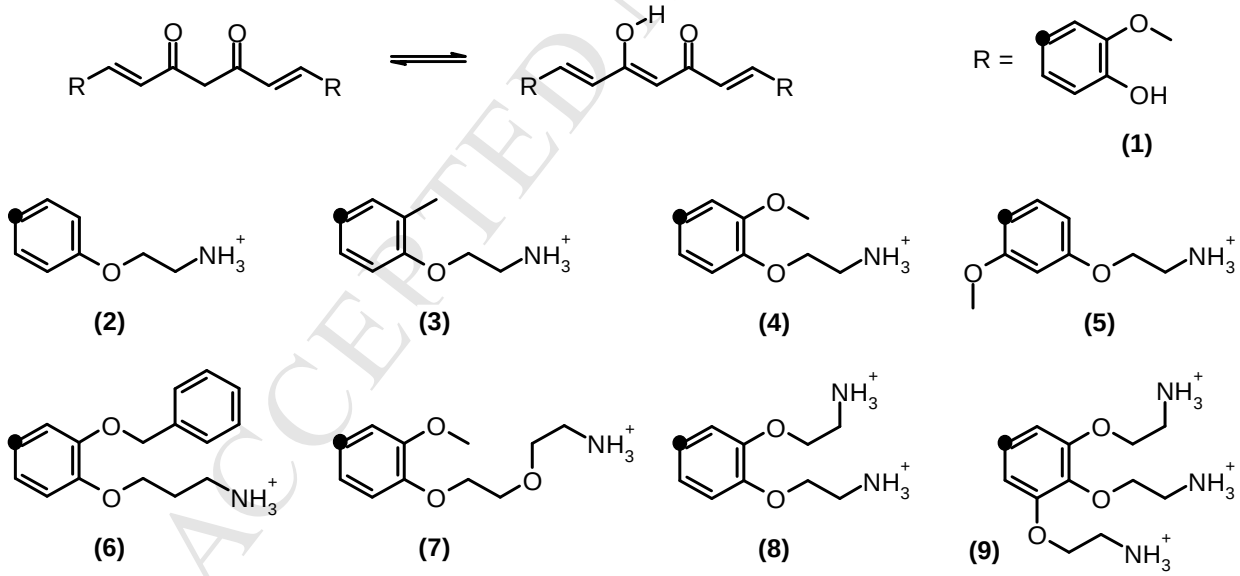


**Figure 1:** The parent compound in its tautomeric forms (**1**) and curcumin derivatives investigated in this study (**2** – **9**); all compounds were prepared as chloride salts

The starting materials for the synthesis are prepared by the substitution of hydroxybenzaldehydes with an alkyl bromide or tosylate in N,N-dimethylformamide (DMF) at elevated temperature:

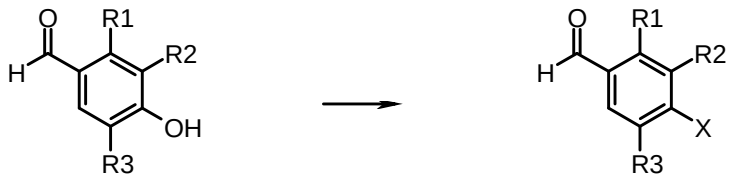


| | | | |
|---|---|---|---|
| **(10)** | R1 = R2 = R3 = H | **(17)** | R1 = R2 = R3 = H<br>X = $OCH_2CH_2NHBoc$ |
| **(11)** | R1 = R3 = H, R2 = Me | **(18)** | R1 = R3 = H, R2 = Me<br>X = $OCH_2CH_2NHBoc$ |
| **(12)** | R1 = R3 = H, R2 = OMe | **(19)** | R1 = R3 = H, R2 = OMe<br>X = $OCH_2CH_2NHBoc$ |
| **(13)** | R2 = R3 = H, R1 = OMe | **(20)** | R2 = R3 = H, R1 = OMe<br>X = $OCH_2CH_2NHBoc$ |
| **(14)** | R1 = R3 = H, R2 = OBz | **(21)** | R1 = R3 = H, R2 = OBz<br>X = $OCH_2CH_2$ $CH_2NHBoc$ |
| **(12)** | R1 = R3 = H, R2 = OMe | **(22)** | R1 = R3 = H, R2 = OMe<br>X = $(OCH_2CH_2)_2NHBoc$ |
| **(15)** | R1 = R3 = H, R2 = OH | **(23)** | R1 = R3 = H, R2 = X = $OCH_2CH_2NHBoc$ |
| **(16)** | R1 = H, R2 = R3 = OH | **(24)** | R1 = H, R2 = R3 = X = $OCH_2CH_2NHBoc$ |

**a** → (10), (11), (12), (13), (15), (16)

**b** → (14)

**c** → (12)

**Scheme 1:** Synthesis of the substituted aldehydes; *conditions: a) $BocHNCH_2CH_2Br$, DMF, $K_2CO_3$, KI, 80°C, overnight, 61 - 87 %; b) $TsOCH_2CH_2OCH_2CH_2NHBoc$, DMF, $K_2CO_3$, KI, 80°C, overnight, 72 %; c) $BocHNCH_2CH_2Br$, DMF, $K_2CO_3$, KI, 80°C, overnight, 84 %;*

Synthesis of the protected curcumin derivatives was performed analog to the common approach via aldehyde/acetylacetone in presence of boric anhydride[41] (Scheme 2) and, starting directly from curcumin using the Mitsonubo reaction [42] (Scheme 3).

Purification of the deprotected derivatives was achieved by precipitation with diethylether and re-precipitation from dichloromethane with diethylether, until the UV/Vis spectra showed constant absorption.

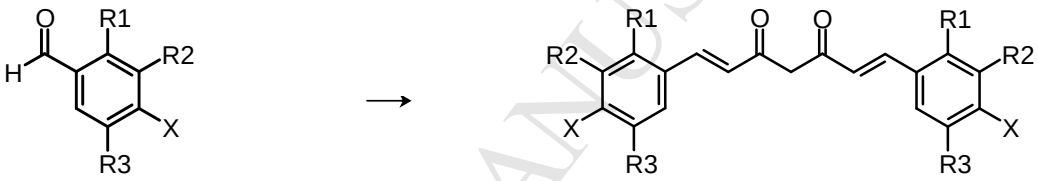


| | R1 = | R2 = | R3 = | X = | | | X = | | | X = |
|---|---|---|---|---|---|---|---|---|---|---|
| **(17)** | H | H | H | $OCH_2CH_2NHBoc$ | | **(25)** | $OCH_2CH_2NHBoc$ | | **(2)** | $OCH_2CH_2NH_3^+$ |
| **(18)** | H | Me | H | $OCH_2CH_2NHBoc$ | | **(26)** | $OCH_2CH_2NHBoc$ | | **(3)** | $OCH_2CH_2NH_3^+$ |
| **(19)** | H | OMe | H | $OCH_2CH_2NHBoc$ | **a** | **(27)** | $OCH_2CH_2NHBoc$ | **b** | **(4)** | $OCH_2CH_2NH_3^+$ |
| **(20)** | OMe | H | H | $OCH_2CH_2NHBoc$ | | **(28)** | $OCH_2CH_2NHBoc$ | | **(5)** | $OCH_2CH_2NH_3^+$ |
| **(21)** | H | OBz | H | $OCH_2CH_2CH_2NHBoc$ | | **(29)** | $OCH_2CH_2CH_2NHBoc$ | | **(6)** | $OCH_2CH_2\ CH_2NH_3^+$ |
| **(22)** | H | OMe | H | $(OCH_2CH_2)_2NHBoc$ | | **(30)** | $(OCH_2CH_2)_2NHBoc$ | | **(7)** | $(OCH_2CH_2)_2NH_3^+$ |

| | R1 = R3 = | R2 = X = | | R2 = X = | | R2 = X = |
|---|---|---|---|---|---|---|
| **(23)** | H | $OCH_2CH_2NHBoc$ | **a** | **(31)** $OCH_2CH_2NHBoc$ | **b** | **(8)** $OCH_2CH_2NH_3^+$ |

| | R1 = | R2 = R3 = X = | | R2 = R3 = X = | | R2 = R3 = X = |
|---|---|---|---|---|---|---|
| **(24)** | H | $OCH_2CH_2NHBoc$ | **a** | **(32)** $OCH_2CH_2NHBoc$ | **b** | **(9)** $OCH_2CH_2NH_3^+$ |

**Scheme 2:** Synthesis and deprotection of the substituted curcumins (**25**–**32**) and their deprotection; *conditions: a) Ethyl acetate, $H_3BO_3$, $B(OBu)_3$, $BuNH_2$, 80°C, 5 h, 41 – 87 %; b) TFA, DCM, RT, 5 h, quant.; then ion exchanger Amberlite IRA-958, water, MeCN*

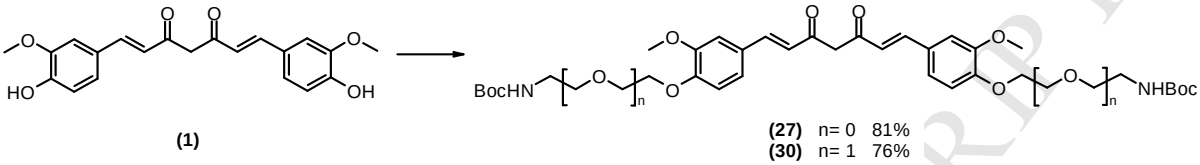


**Scheme 3:** Substitution of curcumin by Mitsonubo reaction; *conditions: THF, DEAD, $PPh_3$, RT, overnight*

The purity of all synthesized compounds was determined by NMR spectroscopic methods (Bruker Avance 300, DMSO-d6) and HPLC-MS confirming a purity of > 97%. $^1$H-NMR spectra of selected compounds and the synthesis procedure for **17** – **24** can be found in the supporting information.

***General procedure 1: Substitution of curcumin by Mitsonubo reaction***

The reaction was conducted under subdued light. Curcumin (0.36 g, 1 mmol), triphenylphosphine (1.04 g, 4 mmol) and the boc-protected aminoalcohol (3 mmol) were dissolved in dry THF (4 mL). DEAD (0.7 g, 4 mmol, 40% in toluene) diluted with dry THF (6 mL) was added dropwise over the course of 20 mins at 2-5 °C. The reaction mixture was stirred for additional 30 mins in the ice bath, then 4 h at room temperature.

Ethyl acetate (40 mL) was added, the organic layer was washed with water (20 mL) trice, separated and dried over $MgSO_4$. All volatiles were removed at reduced pressure and the residue was purified by column chromatography with silica gel and acetone / petroleum ether as the eluent (dryload with acetone). The product was dissolved in the minimum amount of

ethyl acetate and precipitated by slow addition of the tenfold volume of petroleum ether. The orange powder was filtered off and washed with petroleum ether.

*Compound (**27**)*

2-(N-tert-butoxycarbonyl-amino)ethanol (483 mg, 3 mmol) was reacted to yield an orange solid (465 mg, 71% yield). The product was purified with acetone / petroleum ether 1:3 → 1:2 as the eluent.

*Compound (**30**)*

2-(2-(N-tert-butoxycarbonyl-amino)ethoxy)ethanol (715 mg, 3 mmol) was reacted to give an orange solid (386 mg, 52% yield). The product was purified with acetone / petroleum ether 1:2 → 2:3 as the eluent.

***General procedure 2***

Acetylacetone (0.1 g, 1 mmol) and $B_2O_3$ (0.07 g, 1 mmol) are stirred in dried ethyl acetate (2 mL) for 30 mins at 50°C. The substituted aldehyde (20 mmol) in ethyl acetate (3 mL) is added, followed by tri-n-butyl borate (0.7 g, 3 mmol) and stirring is continued for 30 mins at 50°C. n-Butylamine (0.1 mL in 1 mL ethyl acetate) was added dropwise over 5 mins. After 5 h of stirring at 50°C the mixture is allowed to stand overnight at room temperature.

Ethyl acetate (30 mL) is added followed by 60 mL of diluted acetic acid (50 %). For hydrolysis of the borium complex the mixture is stirred for 12 h at room temperature avoiding illumination. The solvents are evaporated at reduced pressure. The residue is extracted with trice with ethyl acetate (30 mL). The combined organic extracts are washed with water (50 mL), dried over $MgSO_4$ and evaporated. The residue was purified by column chromatography with silica gel and acetone / petroleum ether 1:3 → 2:3 as the eluent (dryload with acetone), if

not stated otherwise. The product was dissolved in the minimum amount of ethyl acetate and precipitated by slow addition of the tenfold volume of petroleum ether. The orange powder was filtered off and washed with petroleum ether.

*[2-(4-{7-[4-(2-tert-Butoxycarbonylamino-ethoxy)-phenyl]-3,5-dioxo-hepta-1,6-dienyl}-phenoxy)-ethyl]-carbamic acid tert-butyl ester (**25**)*

Compound **17** (530 mg, 2 mmol) was reacted according to general procedure 2. The product is a yellow solid (363 mg, 61% yield).

**MP** (not corr.) = 136-138°C; - **$^1$H NMR** (300 MHz, $CDCl_3$), δ = 7.61 (d, *J* = 15.8 Hz, 2H), 7.50 (d, *J* = 8.8 Hz, 4H), 6.89 (d, *J* = 8.7 Hz, 4H), 6.50 (d, *J* = 15.8 Hz, 2H), 5.02 (s, 2H), 4.05 (t, *J* = 5.1 Hz, 4H), 3.60 – 3.48 (m, 4H), 1.45 (s, 18H); - **MS** (ESI, $CH_2Cl_2$/MeOH + 10 mmol $NH_4OAc$): 595.3 (100%, $MH^+$), 539.2 (18%, $MH^+$-$C_4H_9$); - **HRMS** (PI-LSIMS FAB, glycerine): calc. for $(M+H^+)^+$: 595.3014, found: 595.3020; - **Molecular Weight** = 594.71 g/mol; - **Molecular Formula** = $C_{33}H_{42}N_2O_8$

*[2-(4-{7-[4-(2-tert-Butoxycarbonylamino-ethoxy)-3-methoxy-phenyl]-3,5-dioxo-hepta-1,6-dienyl}-2-methoxy-phenoxy)-ethyl]-carbamic acid tert-butyl ester (**27**)*

Using compound **19** (590 mg, 2 mmol) in general procedure 2 the product is isolated as an orange solid (590 mg, 61% yield).

**MP** (not corr.) = 149-151°C; - **$^1$H NMR** (300 MHz, $CDCl_3$), δ = 7.58 (d, *J* = 15.7 Hz, 2H), 7.14 – 6.99 (m, 4H), 6.87 (d, *J* = 8.3 Hz, 2H), 6.48 (d, *J* = 15.8 Hz, 2H), 5.16 (s, 2H), 4.09 (t, *J* = 4.9 Hz, 4H), 3.90 (s, 6H), 3.56 (m, 4H), 1.44 (s, 18H); - **MS** (ESI, $CH_2Cl_2$/MeOH + 10 mmol $NH_4OAc$): 655.3 (100%, $MH^+$), 555.3 (26%, $MH^+$-boc); - **HRMS** (PI-LSIMS FAB, glycerine): calc. for $(M+H^+)^+$: 655.3239, found: 655.3241; - **Molecular Weight** = 654.76 g/mol; - **Molecular Formula** = $C_{35}H_{46}N_2O_{10}$

*[2-(4-{7-[4-(2-tert-Butoxycarbonylamino-ethoxy)-2-methoxy-phenyl]-3,5-dioxo-hepta-1,6-dienyl}-3-methoxy-phenoxy)-ethyl]-carbamic acid tert-butyl ester (**28**)*

Compound **20** (530 mg, 2 mmol) was reacted according to general procedure 2 to give an orange-yellow solid (393 mg, 60% yield).

**MP** (not corr.) = 143-145°C; - **$^1$H NMR** (300 MHz, $CDCl_3$), δ = 7.89 (d, *J* = 16.0 Hz, 2H), 7.47 (d, *J* = 8.5 Hz, 2H), 6.62 (d, *J* = 16.0 Hz, 2H), 6.52 – 6.39 (m, 4H), 4.99 (s, 2H), 4.06 (t, *J* = 5.1 Hz, 4H), 3.88 (s, 6H), 3.55 (m, 4H), 1.45 (s, 18H); - **MS** (ESI, $CH_2Cl_2$/MeOH + 10 mmol $NH_4OAc$): 655.3 (100%, $MH^+$); - **HRMS** (PI-LSIMS FAB, glycerine): calc. for $(M+H^+)^+$: 655.3225, found: 655.3231; - **Molecular Weight** = 654.76 g/mol; - **Molecular Formula** = $C_{35}H_{46}N_2O_{10}$

*[2-(4-{7-[4-(2-tert-Butoxycarbonylamino-ethoxy)-3-methyl-phenyl]-3,5-dioxo-hepta-1,6-dienyl}-2-methyl-phenoxy)-ethyl]-carbamic acid tert-butyl ester (**26**)*

Using compound **18** (559 mg, 2 mmol) in general procedure 2 the product is isolated as an orange solid (442 mg, 71% yield).

**MP** (not corr.) = 139-141°C; - **$^1$H NMR** (300 MHz, $CDCl_3$), δ = 7.59 (d, *J* = 15.8 Hz, 2H), 7.36 (d, *J* = 10.8 Hz, 4H), 6.80 (d, *J* = 8.3 Hz, 2H), 6.49 (d, *J* = 15.8 Hz, 2H), 4.94 (s, 2H), 4.06 (t, *J* = 5.0 Hz, 4H), 3.58 (m, 4H), 2.25 (s, 6H), 1.46 (s, 18H); - **MS** (ESI, $CH_2Cl_2$/MeOH + 10 mmol $NH_4OAc$): 623.3 (100%, $MH^+$), 567.3 (21%, $MH^+$-$C_4H_9$); - **HRMS** (PI-LSIMS FAB, glycerine): calc. for $(M+H^+)^+$: 623.3332, found: 623.3336; - **Molecular Weight** = 622.77 g/mol; - **Molecular Formula** = $C_{35}H_{46}N_2O_8$

*[2-(4-{7-[4-(2-tert-Butoxycarbonylamino-ethoxy)-3-benzyloxy-phenyl]-3,5-dioxo-hepta-1,6-dienyl}-2-benzyloxy-phenoxy)-ethyl]-carbamic acid tert-butyl ester (**29**)*

Compound **21** (738 mg, 2 mmol) was reacted according to general procedure 2 to yield an orange solid (5183 mg, 62% yield).

**MP** (not corr.) = 138-140°C; - **$^1$H NMR** (300 MHz, $CDCl_3$), δ = 7.55 (d, *J* = 15.8 Hz, 2H), 7.45 – 7.31 (m, 10H), 7.14 – 7.04 (m, 4H), 6.86 (d, *J* = 8.3 Hz, 2H), 6.46 (d, *J* = 15.8 Hz, 2H), 5.39 (s, 2H), 5.22 (s, 4H), 4.14 (t, *J* = 5.9 Hz, 4H), 3.39 (m, 4H), 2.09 – 2.00 (m, 4H), 1.41 (s, 18H); - **MS** (ESI, $CH_2Cl_2$/MeOH + 10 mmol $NH_4OAc$): 857.4 (100%, $MNa^+$), 835.4 (76%, $MH^+$), 735.4 (53%, $MH^+$-boc); - **HRMS** (PI-LSIMS FAB, glycerine): calc. for $(M+H^+)^+$: 835.4178, found: 835.4179; - **Molecular Weight** = 835.02 g/mol; - **Molecular Formula** = $C_{49}H_{58}N_2O_{10}$

*(2-{2-[4-(7-{4-[2-(2-tert-Butoxycarbonylamino-ethoxy)-ethoxy]-3-methoxy-phenyl}-3,5-dioxo-hepta-1,6-dienyl)-2-methoxy-phenoxy]-ethoxy}-ethyl)-carbamic acid tert-butyl ester (**30**)*

Reaction of compound **22** (530 mg, 2 mmol) by general procedure 2 yields an orange yellow solid as the product (349 mg, 47% yield). The eluent for purification by column chromatography was acetone / petroleum ether 1:2 → 1:1.

**MP** (not corr.) = 105-107°C; - **$^1$H NMR** (300 MHz, $CDCl_3$), δ = 7.59 (d, *J* = 15.8 Hz, 2H), 7.18 – 7.03 (m, 4H), 6.90 (d, *J* = 8.3 Hz, 2H), 6.49 (d, *J* = 15.8 Hz, 2H), 5.07 (s, 2H), 4.24 – 4.15 (m, 4H), 3.91 (s, 6H), 3.88 – 3.83 (m, 4H), 3.61 (t, *J* = 5.1 Hz, 4H), 3.33 (m, 4H), 1.43 (s, 18H); - **MS** (ESI, $CH_2Cl_2$/MeOH + 10 mmol $NH_4OAc$): 671.3 (51%, $MNa^+$), 655.3 (86%, $MH^+$), 555.3 (100%, $MH^+$-boc); - **HRMS** (PI-LSIMS FAB, glycerine): calc. for $(M+H^+)^+$:

743.3750, found: 743.3752; - **Molecular Weight** = 742.87 g/mol; - **Molecular Formula** = $C_{39}H_{54}N_2O_{12}$

*{2-[4-{7-[3,4-Bis-(2-tert-butoxycarbonylamino-ethoxy)-phenyl]-3,5-dioxo-hepta-1,6-dienyl}-2-(2-tert-butoxycarbonylamino-ethoxy)-phenoxy]-ethyl}-carbamic acid tert-butyl ester (**31**)*

Compound **23** (850 mg, 2 mmol) was reacted according to general procedure 2. The product is an orange-red solid (374 mg, 41% yield). The eluent for purification by column chromatography was acetone / petroleum ether 1:3 → 1:2.

**MP** (not corr.) = 95-97°C; - **$^1$H NMR** (300 MHz, $CDCl_3$), δ = 7.57 (d, *J* = 15.8 Hz, 2H), 7.19 – 7.12 (m, 4H), 6.98 – 6.86 (m, 2H), 6.50 (d, *J* = 15.8 Hz, 2H), 5.28 (s, 4H), 4.10 (t, *J* = 4.4 Hz, 8H), 3.55 (m, 8H), 1.46 (s, 18H), 1.45 (s, 18H); - **MS** (ESI, $CH_2Cl_2$/MeOH + 10 mmol $NH_4OAc$): 913.5 (100%, $MH^+$), 457.3 (7%, $(M+2H^+)^{2+}$); - **HRMS** (PI-LSIMS FAB, glycerine): calc. for $(M+H^+)^+$: 913.4810, found: 913.4812; - **Molecular Weight** = 913.08 g/mol; - **Molecular Formula** = $C_{47}H_{68}N_4O_{14}$

*{2-[4-{7-[3,4,5-Tris-(2-tert-butoxycarbonylamino-ethoxy)-phenyl]-3,5-dioxo-hepta-1,6-dienyl}-2,6-bis-(2-tert-butoxycarbonylamino-ethoxy)-phenoxy]-ethyl}-carbamic acid tert-butyl ester (**32**)*

Compound **24** (1166 mg, 2 mmol) was submitted to reaction by general procedure 2. The product is an orange solid (554 mg, 45% yield). The eluent for purification by column chromatography was acetone / petroleum ether 1:4 → 1:2.

**MP** (not corr.) = 90-92°C; - **$^1$H NMR** (300 MHz, $CDCl_3$), δ = 7.52 (d, *J* = 15.1 Hz, 2H), 6.79 (s, 4H), 6.51 (d, *J* = 15.1 Hz, 2H), 5.75 (s, 2H), 5.25 (s, 3H), 4.10 (m, 12H), 3.57 (m, 8H), 3.41 (m, 4H), 1.47 (s, 18H), 1.47 (s, 36H); - **MS** (ESI, $CH_2Cl_2$/MeOH + 10 mmol $NH_4OAc$):

1253.6 (100%, $MNa^+$), 1231.6 (49%, $MH^+$), 1131.3 (51%, $MH^+$-boc); - **HRMS** (PI-LSIMS FAB, glycerine): calc. for $(M+H^+)^+$: 1231.6596, found: 1231.6594; - **Molecular Weight =** 1231.46 g/mol; - **Molecular Formula** = $C_{61}H_{94}N_6O_{20}$

**General procedure 3**

The whole reaction and purification sequence was conducted under protection from light. The boc-protected curcumin (0.2 mmol) was dissolved in dichloromethane (10 mL, dried over $CaCl_2$). Trifluoroacetic acid in dichloromethane (10%, 2.7 mL, 2.4 mmol) cont. TIS (5%) was added dropwise. After stirring for 4 h at room temperature under moisture protection, the suspension was partitioned between six blue caps and diethylether was added to a total volume of 15 mL per cap. The product was settled with the aid of a centrifuge (60 mins, 4400 rpm, 0°C) and the supernatant was discarded. The precipitate was re-suspended in diethylether, settled again and the supernatant was decanted off. This washing step was repeated once using diethylether. Afterwards the product was dried at reduced pressure to give yellow powder.

A small column was packed with ion exchanger (Amberlite IRA-958). The resin was rinsed with acidic sodium chloride solution (10 % aqueous NaCl cont. 0.1 % HCl, 100 mL) washed salt free with dilute hydrochloric acid (0.1 %) and conditioned with dilute hydrochloric acid (0.1 %) / methanol / acetonitrile 9:2:1.

The curcumin TFA salt (0.2 mmol) was dissolved in dilute hydrochloric acid (0.1 %) / methanol / acetonitrile 9:2:1 (2 mL) and was slowly passed through the column (height 10 cm, diameter 1 cm; transferred with 2x 2 mL eluent) of the conditioned anion exchanger (Amberlite IRA-958) eluting with dilute hydrochloric acid (10 mL, 0.1 %). The aqueous solution was lyophilized to give the product as yellow-orange solid.

(1E,6E)-1,7-bis(4-(2-aminoethoxy)phenyl)hepta-1,6-diene-3,5-dione hydrochloride (**2**)

Deprotection of compound **25** yields a yellow powder (93 mg, 0.2 mmol, quant.).

**MP** (not corr.) > 200°C (decomp.); - **$^1$H NMR** (300 MHz, MeOD), δ = 7.60 (m, 6H), 7.04 (d, *J* = 6.9 Hz, 4H), 6.67 (d, *J* = 13.8 Hz, 2H), 4.32 – 4.17 (m, 4H), 3.46 – 3.34 (m, 4H); - **MS** (ESI, MeCN/$H_2O$ + 0.06 % TFA): 198.1 (100%, $(M+2H^+)^{2+}$), 352.2 (9%, $MH^+$ -$C_2H_5N$), 395.2 (2%, $MH^+$); - **HRMS** (PI-LSIMS FAB, glycerine): calc. for $(M+2H^+)^{2+}$: 198.1019, found: 198.1028; - **Molecular Weight =** 467.39 g/mol; - **Molecular Formula** = $C_{23}H_{28}N_2O_4Cl_2$

(1E,6E)-1,7-bis(4-(2-aminoethoxy)-3-methylphenyl)hepta-1,6-diene-3,5-dione hydrochloride (**3**)

Deprotection of compound **26** yields an orange powder (91 mg, 0.183 mmol, 92 %)

**MP** (not corr.) > 200°C (decomp.); - **$^1$H NMR** (300 MHz, MeOD), δ = 7.60 (d, 14.3 Hz, 2H), 7.55 – 7.37 (m, 4H), 6.99 (d, *J* = 6.8 Hz, 2H), 6.68 (d, *J* = 14.3 Hz, 2H), 4.28 (m, 4H), 3.48 – 3.39 (m, 4H), 2.31 (s, 6H); - **MS** (ESI, MeCN/$H_2O$ + 0.06 % TFA): 212.1 (100%, $(M+2H^+)^{2+}$), 380.2 (6%, $MH^+$ -$C_2H_5N$), 423.2 (2%, $MH^+$); - **HRMS** (PI-LSIMS FAB, glycerine): calc. for $(M+2H^+)^{2+}$: 212.1176, found: 212.1173; - **Molecular Weight =** 495.44 g/mol; - **Molecular Formula** = $C_{25}H_{32}N_2O_4Cl_2$

(1E,6E)-1,7-bis(4-(2-aminoethoxy)-3-methoxyphenyl)hepta-1,6-diene-3,5-dione hydrochloride (**4**)

Deprotection of compound **27** yields a yellow powder (94 mg, 0.178 mmol, 89 %)

**MP** (not corr.) > 200°C (decomp.); - **$^1$H NMR** (300 MHz, MeOD), δ = 7.61 (d, *J* = 15.7 Hz, 2H), 7.33 (s, 2H), 7.23 (d, *J* = 8.2 Hz, 2H), 7.06 (d, *J* = 8.2 Hz, 2H), 6.74 (d, *J* = 15.7 Hz, 2H), 6.03 (s, 1H), 4.33 – 4.22 (m, 4H), 3.95 (s, 6H), 3.45 – 3.34 (m, 4H); - **MS** (ESI, MeCN/$H_2O$ + 0.06 % TFA): 228.1 (100%, $(M+2H^+)^{2+}$), 412.2 (5%, $MH^+$ -$C_2H_5N$), 455.2 (3%, $MH^+$); - **HRMS** (PI-LSIMS FAB, glycerine): calc. for $(M+2H^+)^{2+}$: 228.1125, found: 228.1133; - **Molecular Weight =** 527.44 g/mol; - **Molecular Formula** = $C_{25}H_{32}N_2O_6Cl_2$

(1E,6E)-1,7-bis(4-(2-aminoethoxy)-2-methoxyphenyl)hepta-1,6-diene-3,5-dione hydrochloride (**5**)

Deprotection of compound **28** yields a yellow powder (92 mg, 0.174 mmol, 87 %)

**MP** (not corr.) > 200°C (decomp.); - **$^1$H NMR** (300 MHz, MeOD), δ = 7.63 (d, *J* = 15.8 Hz, 2H), 7.52 -7.02 (m, 6H), 6.77 (d, *J* = 15.7 Hz, 2H), 4.35 – 4.25 (m, 4H), 3.87 (s, 6H), 3.42 – 3.32 (m, 4H); - **MS** (ESI, MeCN/$H_2O$ + 0.06 % TFA): 228.1 (100%, $(M+2H^+)^{2+}$), 412.2 (5%, $MH^+$ -$C_2H_5N$), 455.2 (3%, $MH^+$); - **HRMS** (PI-LSIMS FAB, glycerine): calc. for $(M+2H^+)^{2+}$: 228.1128, found: 228.1133; - **Molecular Weight =** 527.44 g/mol; - **Molecular Formula** = $C_{25}H_{32}N_2O_6Cl_2$

(1E,6E)-1,7-bis(4-(3-aminopropoxy)-3-(benzyloxy)phenyl)hepta-1,6-diene-3,5-dione hydrochloride (**6**)

Deprotection of compound **29** yields an orange powder (106 mg, 0.150 mmol, 75%)

**MP** (not corr.) > 175°C (decomp.); - **$^1$H NMR** (300 MHz, MeOD), δ = 7.57 (m, 2H), 7.48 – 7.33 (m, 12H), 7.28 (m, 2H), 7.08 (m, 2H), 6.68 (m, 2H), 5.13 (s, 4H), 4.23 (m, 4H), 3.16 (t, *J* = 6.4 Hz, 4H), 2.16 (m, 4H); - **MS** (ESI, MeCN/$H_2O$ + 0.06 % TFA): 286.1 (100%, $(M+2H^+)^{2+}$), 545.3 (4%, $MH^+$ -$C_2H_5N$), 635.3 (1%, $MH^+$); - **HRMS** (PI-LSIMS FAB,

glycerine): calc. for $(M+2H^+)^{2+}$: 318.1594, found: 318.1605; - **Molecular Weight =** 707.7 g/mol; - **Molecular Formula** = $C_{39}H_{44}N_2O_6Cl_2$

(1E,6E)-1,7-bis(4-(2-(2-aminoethoxy)ethoxy)-3-methoxyphenyl)hepta-1,6-diene-3,5-dione hydrochloride (**7**)

Deprotection of compound **30** yields a yellow sticky solid (107 mg, 0.174 mmol, 92 %).

**MP** (not corr.) = 118 - 120°C; - **$^1$H NMR** (300 MHz, MeOD), δ = 7.60 (d, *J* = 15.7 Hz, 2H), 7.28 (s, 2H), 7.20 (d, *J* = 8.2 Hz, 2H), 7.01 (d, *J* = 8.3 Hz, 2H), 6.70 (d, *J* = 15.8 Hz, 2H), 4.22 (dd, *J* = 5.2, 3.3 Hz, 4H), 3.91 (s, 6H), 3.94 – 3.88 (m, 4H), 3.83 – 3.76 (m, 4H), 3.16 (t, *J* = 3.2 Hz, 4H); - **MS** (ESI, MeCN/$H_2O$ + 0.06 % TFA): 272.1 (100%, $(M+2H^+)^{2+}$), 500.2 (3%, $MH^+$ -$C_2H_5N$), 543.3 (3%, $MH^+$); - **HRMS** (PI-LSIMS FAB, glycerine): calc. for $(M+2H^+)^{2+}$: 272.1387, found: 272.1397; - **Molecular Weight =** 615.55 g/mol; - **Molecular Formula** = $C_{29}H_{40}N_2O_8Cl_2$

(1E,6E)-1,7-bis(3,4-bis(2-aminoethoxy)phenyl)hepta-1,6-diene-3,5-dione hydrochloride (**8**)

Deprotection of compound **31** yields an orange powder (118 mg, 0.179 mmol, 90 %)

**MP** (not corr.) > 166°C (decomp.); - **$^1$H NMR** (300 MHz, MeOD), δ = 7.61 (d, *J* = 15.8 Hz, 2H), 7.37 (s, 2H), 7.35 – 7.28 (m, 2H), 7.10 (d, *J* = 8.4 Hz, 2H), 6.74 (d, *J* = 15.8 Hz, 2H), 6.02 (s, 1H), 4.32 (dd, *J* = 9.8, 4.9 Hz, 8H), 3.43 (t, *J* = 4.8 Hz, 8H); - **MS** (ESI, MeCN/$H_2O$ + 0.06 % TFA): 171.8 (100%, $(M+3H^+)^{3+}$), 235.6 (43%, $(M+2H^+)^{2+}$ -$C_2H_5N$), 257.1 (44%, $(M+2H^+)^{2+}$), 513.3 (15%, $MH^+$); - **HRMS** (PI-LSIMS FAB, glycerine): calc. for $(M+2H^+)^{2+}$: 257.1396, found: 257.1388; - **Molecular Weight =** 658.44 g/mol; - **Molecular Formula** = $C_{27}H_{40}N_4O_6Cl_4$

(1E,6E)-1,7-bis(3,4,5-tris(2-aminoethoxy)phenyl)hepta-1,6-diene-3,5-dione hydrochloride (**9**)

Deprotection of compound **32** yields an orange powder (141 mg, 0.166 mmol, 83 %)

**MP** (not corr.) > 160°C (decomp.); - **$^1$H NMR** (300 MHz, MeOD), δ = 7.62 (d, *J* = 15.8 Hz, 2H), 7.12 (s, 4H), 6.84 (d, *J* = 15.9 Hz, 2H), 4.41 – 4.29 (m, 8H), 4.27 – 4.20 (m, 4H), 3.50 – 3.40 (m, 8H), 3.39 – 3.33 (m, 4H); - **MS** (ESI, MeCN/$H_2O$ + 0.06 % TFA): 158.6 (47%, $(M+4H^+)^{4+}$), 211.1 (100%, $(M+3H^+)^{3+}$), 273.1 (6%, $(M+2H^+)^{2+}$ -$C_2H_5N$), 316.2 (24%, $(M+2H^+)^{2+}$), 631.3 (12%, $MH^+$); - **HRMS** (PI-LSIMS FAB, glycerine): calc. for $(M+2H^+)^{2+}$: 316.1761, found: 316.1771; - **Molecular Weight =** 849.50 g/mol; - **Molecular Formula =** $C_{31}H_{52}N_6O_8Cl_6$

**Absorption and emission spectra.** Each spectrum was recorded in the range from 200 nm to 600 nm in 1 nm steps in a quartz cuvette. The spectrum of blank buffer medium or Millipore water was subtracted.

**Determination of Polarity.** The polarity of the compounds was estimated via their octanol-water partition coefficient at 25 °C by the shake-flask method. 5 mL of 50 µM photosensitizer in 10 mM Sörensen buffer pH 6.8 were mixed with 5 mL of n-octanol and agitated vigorously for 10 min. Both layers were separated using a centrifuge (25°C, 4000 rpm, 5 min). The absorbance of the aqueous solution before and after mixing with n-octanol was measured in a quartz cuvette with a thickness of 10 mm. The partition coefficient was calculated from the concentrations corresponding to these values. In this concentration range the absorbance shows linear behavior. As the absorption intensity of curcumin is dependent on the polarity of

the solvent,[43] only the values for the aqueous solutions were used for calculation of the coefficient.

**Determination of photostability and singlet oxygen quantum yields**

Compound **4** was dissolved in pure water at concentration of 2 µM. For the estimation of the photostability the solution was irradiated with 107 mW in a time span of 20 minutes. Illumination occurred by a tunable laser system (NT242-SH/SFG, Ekspla, Lithania) with a wavelength of 405 nm. Absorption spectra were recorded in distinct time intervals.

The oxygen consumption of the solutions was measured by an oxygen microsensor (Presens, Regensburg, Germany) with a starting concentration of oxygen in water of 270 µM (air saturated).

Singlet oxygen signals were recorded with a high sensitive NIR-system described elsewhere [44-46] using an appropriate laser system . The singlet oxygen signal of 20 seconds was recorded over 20 minutes to estimate the stability of singlet oxygen generation depending on absorption of radiation and the energy transfer from the PS to oxygen in the ground state.

The $^1O_2$ quantum yield $\Phi_\Delta$ of **4** was determined using 5,10,15,20-Tetrakis(1-methyl-4-pyridinio)porphyrin tetra(p-toluenesulfonate) (TMPyP) with a $\Phi_\Delta = 0.77 \pm 0.10$ as a reference PS. [47] Therefore the absorbed energy of a TMPyP solution (c = 0.5 µM) and a solution of **4** (2 µM) were compared to their emitted singlet oxygen luminescence at 1270 nm as described before. [44] Both PS were excited at 405 nm generated by a tunable laser system (NT 242-SH/SFG, Ekspla, Vilnius, Lithuania) with different excitation powers of 107mW, 162mW, 255mW and 283 mW for 50 seconds.

**Experimental procedure for PDI.** All experiments were performed under sterile conditions using a laminar flow bench (Biosafe 4-130, Ehret, Emmendingen, Germany). After adding the

photosensitizer experimentation was done under subdued light.

**Bacterial strains and growth conditions.** A volume of 20 mL medium was inoculated with *Escherichia coli* (ATCC25922, Manassas,Virginia). The suspension was incubated overnight at 37 °C under constant agitation (175 rpm) on a shaker (MAXQ4000, Thermo Scientific, Dubuque, Iowa, USA). For growing of *E. coli* Todd-Hewittt Bouillon (Carl Roth, Karlsruhe, Germany) with a supplement of 0.3 % yeast extract (AppliChem, Darmstadt, Germany) was used as medium.

The volume of overnight culture was diluted to 20 mL bacterial solution with absorption 0.05 and incubated for two hours at 37 °C under constant agitation (175 rpm) on a shaker. The resulting absorption (600 nm) was between 0.3 and 0.45.

*Staphylococcus aureus* (ATCC25923; Manassas,Virginia) was grown aerobically at 37°C in Mueller-Hinton broth (Gibco Life Technologies GmbH, Eggenstein, Germany). Bacteria originated from culture shaking overnight (5 mL) harvested by centrifugation (3000 rpm, 10 min; Megafuge 1.0, Heraeus Sepatech, Osterode, Germany). The cells were resuspended in distilled water at an optical density of 0.6, which was measured at 600 nm with a spectrometer (SPECORD 50 PLUS, Analytik Jena, Jena, Germany) and corresponded to a bacterial count of $10^8$ bacterial cells per mL.

**Light sources and illumination parameters.** Two different systems were used for illumination. A LED light source (consisting of an array of 432 LED 435-12-30, Roithner Lasertechnik, Vienna, Austria) with a wavelength emission of 430 nm – 435 nm was used for phototoxicity experiments screening efficacy with all curcumin derivatives with *E. coli*. The intensity was set to 9.4 mW $cm^{-2}$. A non-coherent light source (Partial Body UV Therapy

System UV 802 L with BlueV tubes; Waldmann AG, Villingen-Schwenningen, Germany) emitting light from 380 nm – 480 nm was used for follow-up experiments with *S. aureus* and *E. coli*. The intensity was adjusted to 17.5 mW $cm^{-2}$.

The effective radiant exposure of the light sources was calculated as follows:

$$radiant\ exposure\ \left[\frac{J}{cm2}\right] = \frac{power}{area}\ x\ time\ \left[\frac{W}{cm2}\right] x\ s$$

**Photosensitizer solutions.** The photosensitizers used for the bacteria were diluted in distilled water or Dulbecco`s Phosphate Buffered Saline (DPBS) to get the final concentrations 0/1/5/10/25/50/100/250/500 µ$ML^{-1}$.

**Phototoxicity assay against bacteria.** Three different controls were performed for each PS. The “light only” control (LO) was illuminated but not incubated using the medium without photosensitizer. The “photosensitizer only” control (PS only) was incubated with photosensitizer, but was not illuminated. This control was performed with the highest used concentration and longest incubation period and in addition with a concentration and incubation period most preferable for practice use. The “double negative” control (Co-/-) was neither incubated with photosensitizer nor illuminated.

After two hours the culture of *E. coli* was splitted into aliquots of 1800 µL each. Cells were then harvested by centrifugation at 20 °C, 830 rcf, for 5 min (5417R Centrifuge, Eppendorf, Hamburg, Germany) and resuspended in DPBS. Different volumes of the respective photosensitizer stock solution were added to the suspensions, constantly resulting in a final volume of 1800 µL. The obtained suspensions of different photosensitizer concentrations

were again incubated on the shaker immediately (37 °C, 175 rpm; MAXQ4000, Thermo Scientific, Schwerte, Germany). Doublets of 500 µL were transferred into a 24-well microplate (Cellstar, Greiner Bio-One, Frickenhausen, Germany). The PS only and co-/- controls were transferred into a separate microplate wrapped with aluminum foil. Illumination was done with a LED-Array device from the bottom (9.4 mW $cm^{-2}$, 33.8 J $cm^{-2}$), under constant agitation with a shaking device (MTS4, IKA, Staufen, Germany). After illumination dilution series (1:10) were done with DPBS. Fifty microliters of each dilution step were plated on 1.5 % Agar (Agar-Agar, Kobe I, Roth, Karlsruhe, Germany) with 3 % Todd-Hewitt Bouillon (Carl Roth, Karlsruhe, Germany) and a supplement of 0.3 % yeast extract (AppliChem, Darmstadt, Germany). The inoculated agar plates were incubated at 37 °C overnight and bacterial colonies were counted.

For the follow-up experiments an aqueous solution of approximately $10^8$ *S. aureus* or *E. coli* cells per mL were placed into a 96-well microtiter plate (25 mL each) and incubated with different concentrations of photosensitizer solution. Suspensions were immediately irradiated with 20 mW $cm^{-2}$. Time and dose for the respective experiment are given in the discussion. Aliquots of a serial dilution were plated on Mueller - Hinton agar and incubated for 24 h at 37°C.

The survival of the bacteria was determined by counting the numbers of colony forming units (CFU) 24 h after illumination using the Miles, Misra and Irwin technique. [48] All experiments were replicated at least three times. The relative inactivation was calculated by dividing the CFU count of the double negative control (Co -/-, no incubation with PS and no illumination) by the CFU value of the particular sample. The detection limit was defined as 10 CFU/mL.

## Results & Discussion

### Spectroscopic Characterization and Photophysics

Compounds **2** to **9** were investigated for their photophysical stability and absorption characteristics. All measurements were conducted in Sörensen buffer (0.01 M) at pH = 7. The molar extinction coefficients for compounds **2** to **9** are summarized in table 1.

The di-ketone group in the curcumin structure exhibits keto-enol tautomerism, which can exist in different types of conformers depending on the environment. [49] In aqueous solution the keto-enol form is more stabilized than the diketo form. [50] The intense light absorption maximum ($\lambda_{max}$) at 420 nm is attributed to the keto-enol form and can be assigned to $\pi$–$\pi^*$ transitions, the shoulder at approx. 350 nm to n–$\pi^*$ transitions. Detailed information about the isomeric forms of alkylated curcumin and the impact of the isomerism on the spectra are described elsewhere.[51, 52]

All substances, except **2** and **5**, show comparable absorption characteristics in the range from 410 nm to 430 nm (figure 2). Spectrum of **9** deviates downwards and in comparison to the other curcuminoids, the peak wavelength is about 10 nm blue shifted.

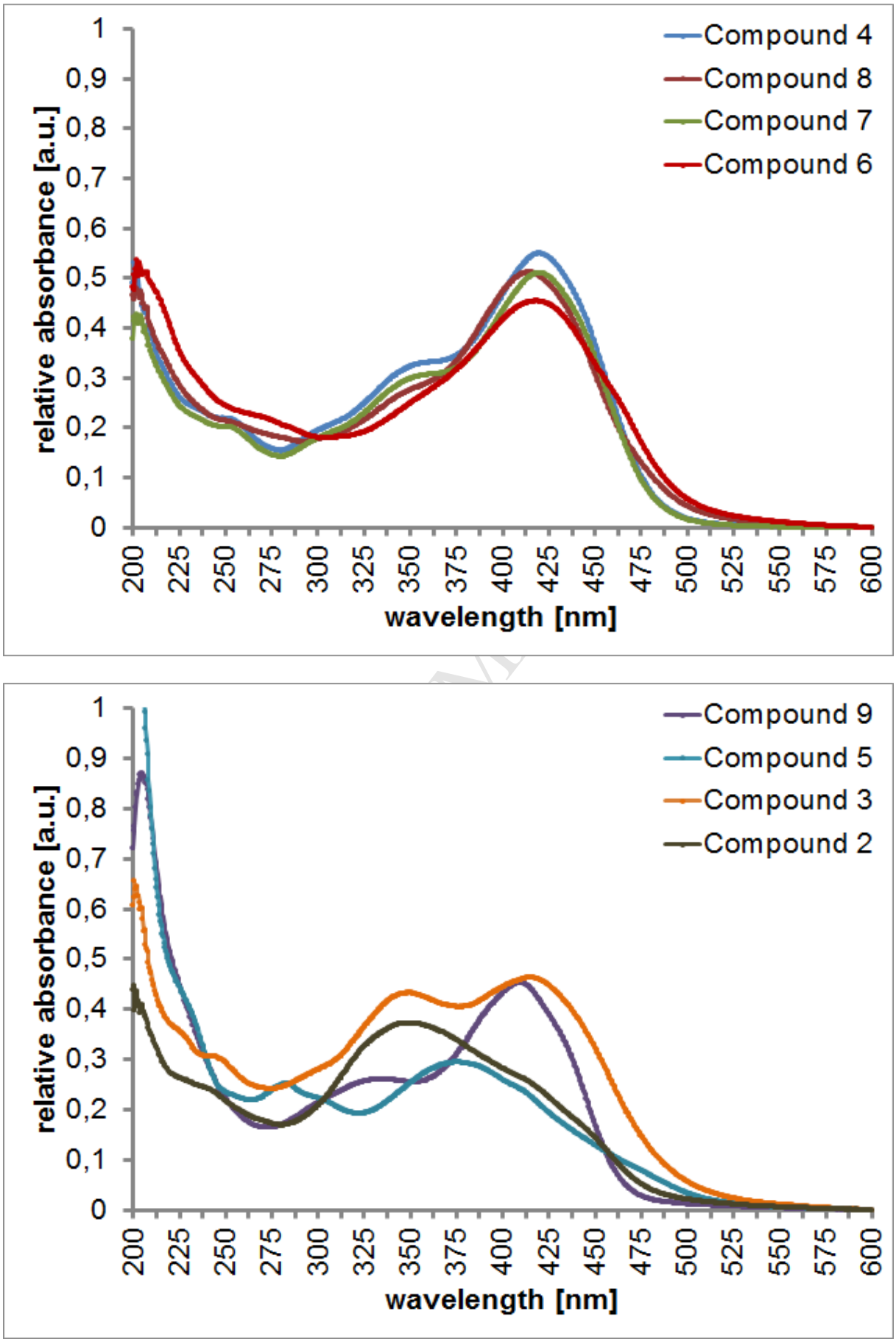


**Figure 2:** absorption spectra of derivatives **2 -9**

The molar extinction coefficients for compounds **3, 4, 6 – 9** ranging from 22000 to 28000 $M^{-1}cm^{-1}$ match or slightly exceed the value given for curcumin in the literature ($\varepsilon_{420,\ H2O}$= 23800 $M^{-1}cm^{-1}$).[53] The absorption maxima of **2** and **5** are blue shifted and ε values obtained are significantly lower (fig. 2 and table 1), which can be explained by the absence of auxochromic groups in **2** and different position of the electron donating methoxy groups in **5** in comparison to other derivatives like **4** or **7**. The experimentally obtained differences in molar extinction coefficients and shifts of the absorption spectra of the derivatives are in good accordance with the literature data for the corresponding dimethoxycurcumins.[54]

The emissions spectra of both light sources and the absorption characteristics of compound **4** as typical example (27600 ± 300 $L \cdot mol^{-1} \cdot cm^{-1}$ within the error margins) is shown in figure 3.

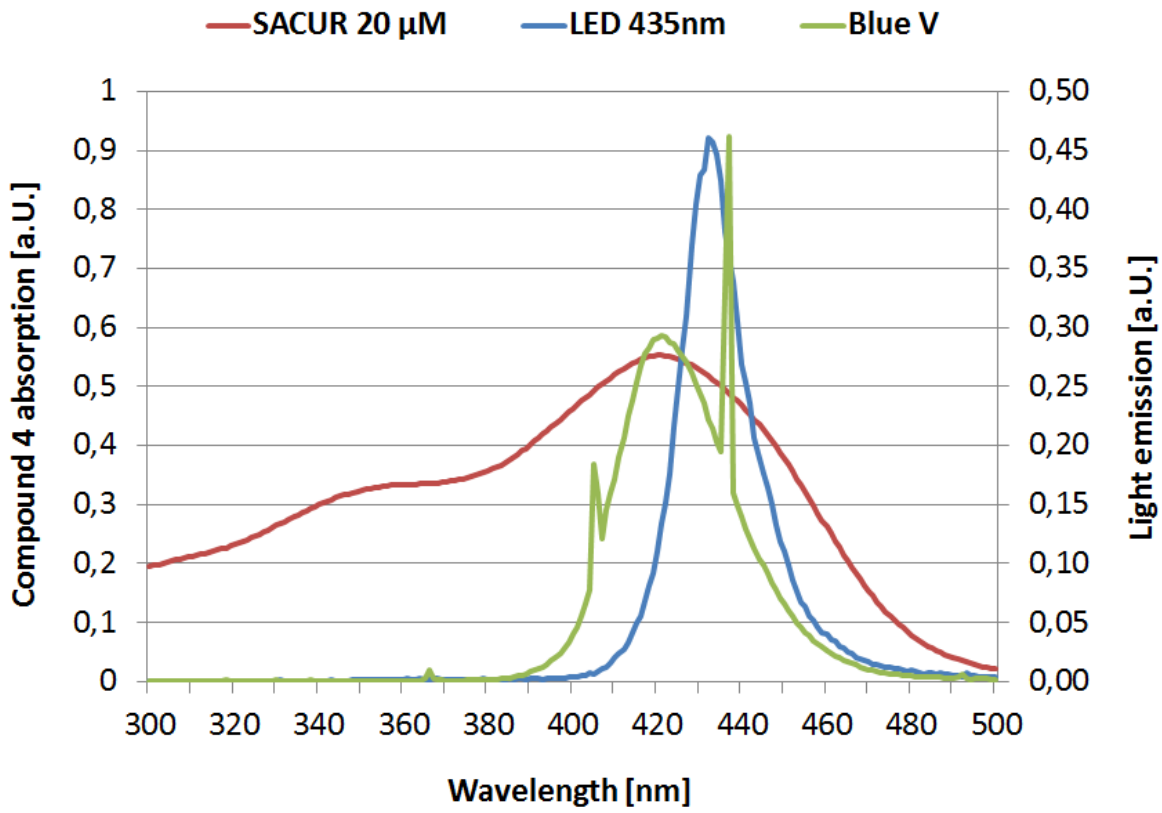


**Figure 3:** Absorption spectrum (red) of **4** overlapping with the emission spectra of the light sources LED 435 nm (blue line) and BlueV (green line; scaled x 1/2)

The emission spectra of both light sources employed in this study without proportion of UV radiation perfectly overlap with the visible region of the curcuminoid spectrum (400 – 470 nm) ensuring an optimal excitation of the photosensitizer.

All compounds showed photodegradation, which was less than 10 % upon illumination with the LED source at 435 nm for 10 minutes, equals an applied dose of 5.6 J/cm², and approx. 20% after 30 minutes, equals an applied dose of 16.9 J/cm². Upon extrapolation of the data the half life time for *SACUR-03* (**8**) was calculated to be approx. 60 min at intensity of 9.4 mW $cm^{-2}$. Figure 4 shows exemplarily the photodegradation of compound **8**. The chromophore signal between 380 and 460 nm was irreversibly decreased in intensity, indicating that the conjugated double bond system between the phenyl rings of the curcuminoid was disrupted and products of smaller molecular weight and lower degrees of conjugation were formed (fig. 4).

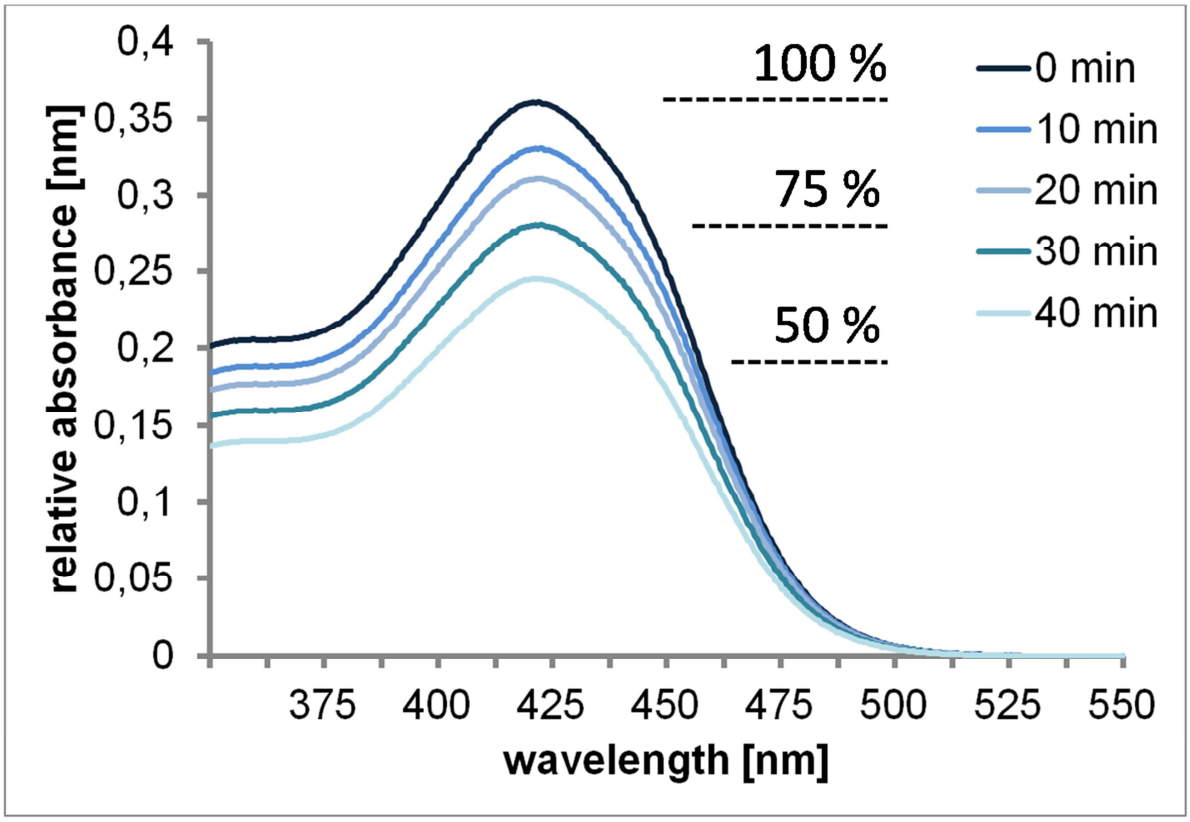

**Figure 4:** Photostability measurements of 10 µM of **8** in water in a quartz cuvette with an illumination at 435 nm with the LED device used for bacterial testing (9.4 mW/cm²); time values in the graphs legend are given in minutes.

Previous studies showing a rapid decomposition of curcumin to vanillin, ferulic acid and feroloyl methane in buffer systems at neutral-basic pH conditions: When curcumin was incubated in 0.1 M phosphate buffer and serum-free medium, pH 7.2 at 37°C, about 90% decomposed within 30 min. The initial degradation products were formed after only a few minutes, and feruloyl methane was then transformed by hydrolysis to the degradation products vanillin and acetone.[55]

The potential pathway for the photodegradation of the curcumin chromophor by involvement of light-induced generated ROS may be explained as follows: The reaction is expected to start with an electrophilic attack of singlet oxygen at one of the double bonds of the molecules **2** to **9** or a radical oxidation process similar to lipid peroxidation in fatty acids [56] leading for example to **38**. (Scheme 4, (b)). The degradation of curcumin in aqueous buffer at physiological pH is an autoxidation reaction.[57] A radical chain reaction leads to incorporation of oxygen into curcumin, resulting in deoxygenated bicyclopentadione products.[58]

We hypothesize the following process takes place in an analog mechanism as described in detail for curcumin [59] (**1**) and dimethoxycurcumin: After illumination a cyclisation product (**37**), as well as decomposition products such as substituted vanillic acids, methoxybenzaldehyde derivatives (**36**) and substituted ferulic acids (**33**) are formed (Scheme 4, (a)).

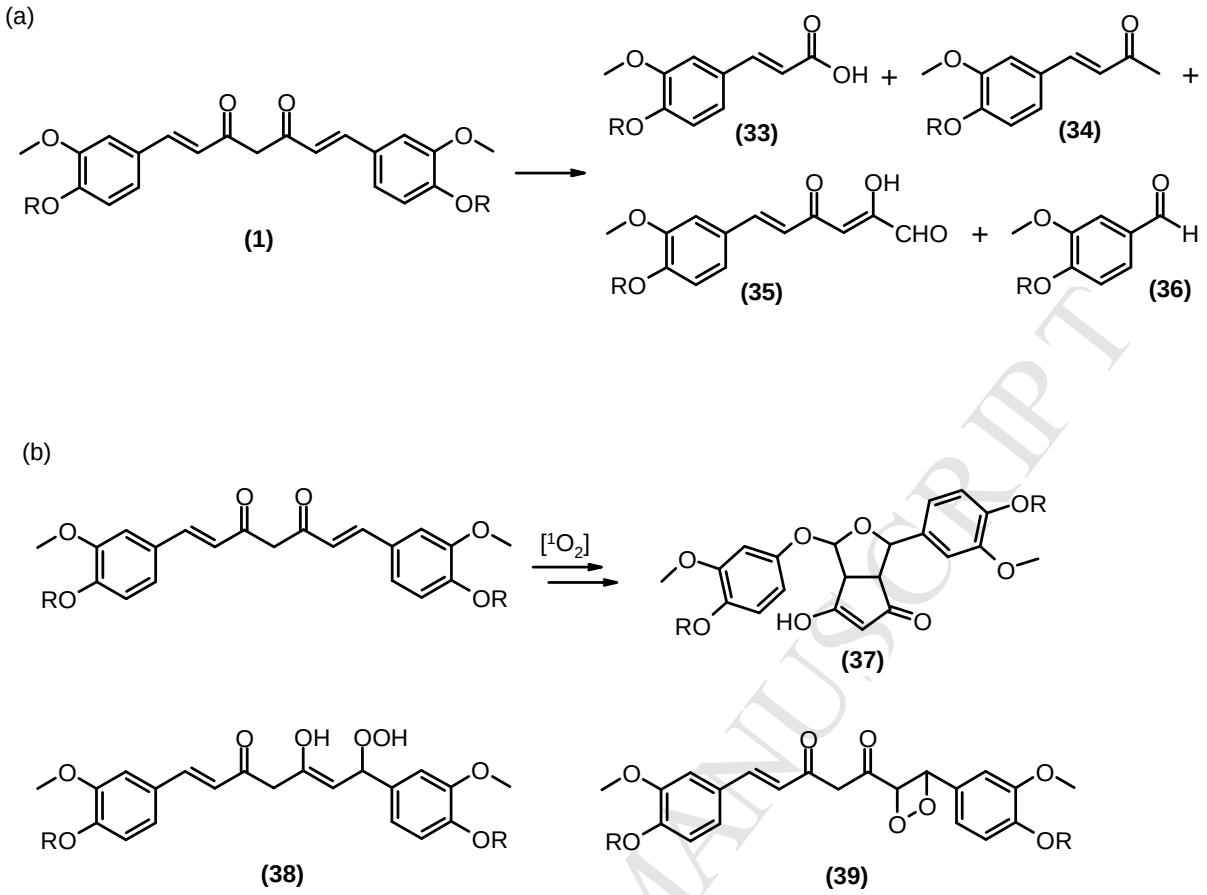


**Scheme 4:** Photodegradation; (a) assumed breakdown main products and (b) postulated oxidation products and intermediates of the photosensitizers

Substitution of the double bond by singlet oxygen results in a cyclic peroxide (**39**) which can be cleaved to the above mentioned products. These processes finally leads to breakdown and bleaching of the chromophor.

The known mechanism [59] of autooxidative degradation of curcumin via phenolic OH groups is hindered in the alkylated curcumin derivatives. This explains the longer half-life of the derivatives **2** – **9**.

All compounds investigated do not show a measurable singlet oxygen luminescence signal (quantum yields $\Phi_\Delta < 1$ %) at 1270 ± 10 nm. This is in good accordance with the literature value ($\Phi_\Delta = 0.011$ in water). [60] Curcumin is known as a ROS generator reacting nearly quantitatively according to Type I photochemical reaction, that is the formation of reactive

oxygen species without generation of singlet oxygen. [61, 62] For spectroscopic data please see the supporting information. We assume the marginal amounts of $^1O_2$ generated by the curcumin derivatives are consumed by reaction with the photosensitizer itself.

**Polarity, pH- and temperature stability**

The polarity of the novel photosensitizers was estimated by measuring the octanol-water partition coefficient. Distribution of $1*10^{-4}$ mol of the chloride salt of each compound between n-octanol and Sörensen buffer (0.01 M, pH = 6.8) was measured by UV/Vis spectroscopy after 10 minutes of stirring at room temperature. Table 1 summarizes the results of the physical parameters of the phenalen-1-one derivatives:

| Photosensitizer 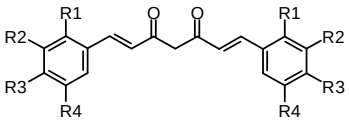 | | $\lambda_{max}$ absorption [nm]$^{(a)}$ | molar extinction coefficient $\varepsilon^{(a)}$ [$L \cdot mol^{-1} \cdot cm^{-1}$] | $\lambda_{max}$ emission [nm] $^{(a)}$ | octanol / water coefficient log D $^{(b)}$ |
|---|---|---|---|---|---|
| Residue | | | | | |
| R1 = R2 = R4 = H, R3 = $OCH_2CH_2NH_3^+$ | (**2**) | 350 ± 2 | 18600 ± 200 | 525 ± 5 | -0.9 ± 0.2 |
| R1 = R4 = H, R2 = Me, R3 = $OCH_2CH_2NH_3^+$ | (**3**) | 415 ± 2 | 23200 ± 300 | 541 ± 5 | -0.8 ± 0.2 |
| R1 = R4 = H, R2 = OMe, R3 = $OCH_2CH_2NH_3^+$ | (**4**) | 421 ± 2 | 27600 ± 400 | 562 ± 5 | -1.2 ± 0.2 |
| R2 = R4 = H, R1 = OMe, R3 = $OCH_2CH_2NH_3^+$ | (**5**) | 374 ± 2 | 14700 ± 200 | 557 ± 5 | -1.1 ± 0.3 |
| R1 = R4 = H, R2 = OBz, R3 = $OCH_2CH_2NH_3^+$ | (**6**) | 419 ± 2 | 22700 ± 300 | 561 ± 5 | - 0.6 ± 0.1 |
| R1 = R4 = H, R2 = OMe, R3 = $(OCH_2CH_2)_2NH_3^+$ | (**7**) | 423 ± 2 | 25500 ± 300 | 560 ± 5 | -1.6 ± 0.2 |
| R1 = R4 = H, R2 = R3 = $OCH_2CH_2NH_3^+$ | (**8**) | 416 ± 2 | 26100 ± 400 | 556 ± 5 | < - 2.0 |
| R1 =H, R2 = R3 = R4 = $OCH_2CH_2NH_3^+$ | (**9**) | 410 ± 2 | 22600 ± 300 | 567 ± 5 | < - 2.0 |

**Table 1:** Physical parameters of the phenalen-1-one derivatives; conditions: (a) at 25 °C in Millipore water, (b) at 25°C in Sörensen buffer 0.01 M at pH 7

The $pK_a$ value of the ammonium groups was 9.2 ± 0.4 for compound **4**. At a pH of 7 the derivatives are therefore fully protonated.

**Aggregation**

Aggregation of the curcumin photosensitizers was studied exemplarily with compound **4** and **8** over a wide concentration range via UV/Vis spectroscopy (Fig. 5) and NMR studies (Fig. 6). Solvents used were Millipore water (18MΩ) or $D_2O$, respectively. The spectra for compound 8 can be found in the supporting information.

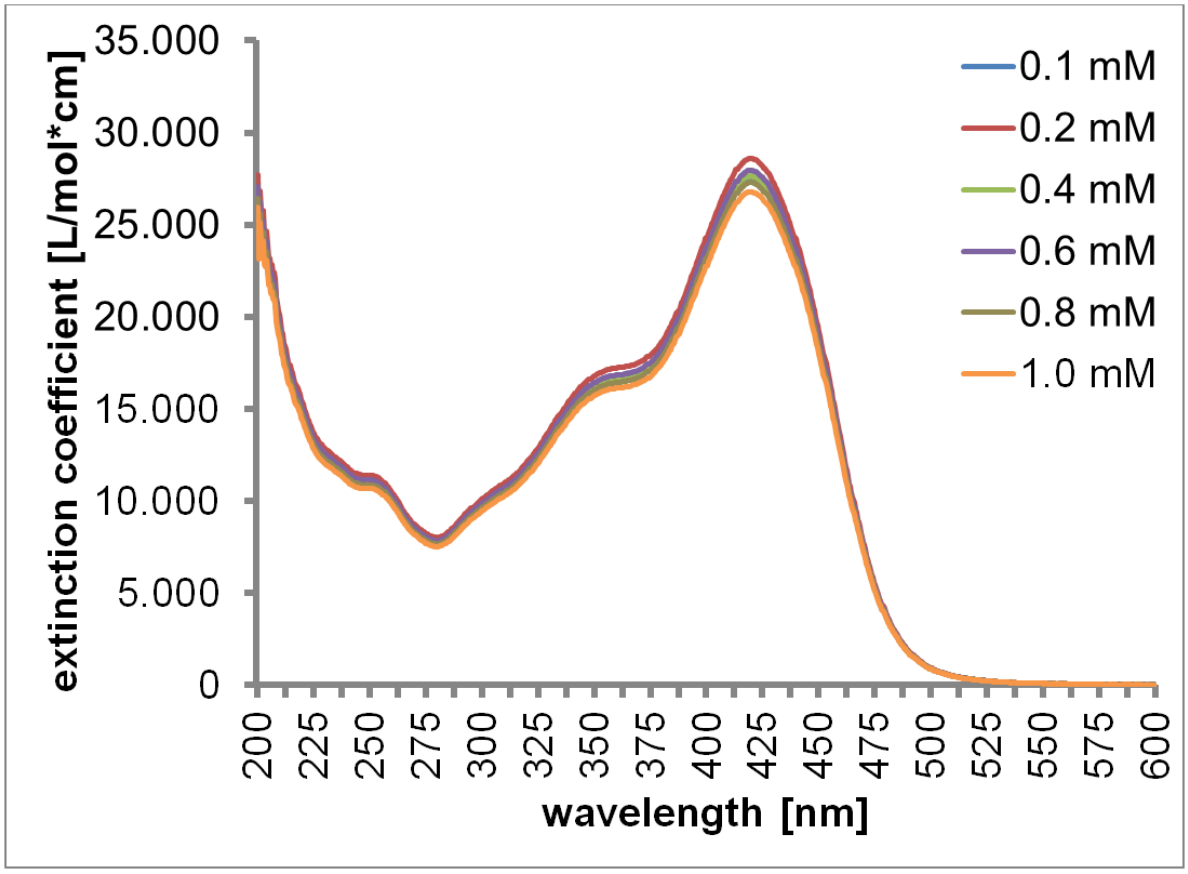


**Figure 5:** Absorption spectra of (**4**) within a concentration range of 100 – 1000 µM in $H_2O$; within the error margins no dimerization can be observed in the concentration range covered.

With compound **8** no dimerization became apparent up to 1 mM (see supporting information for spectra).

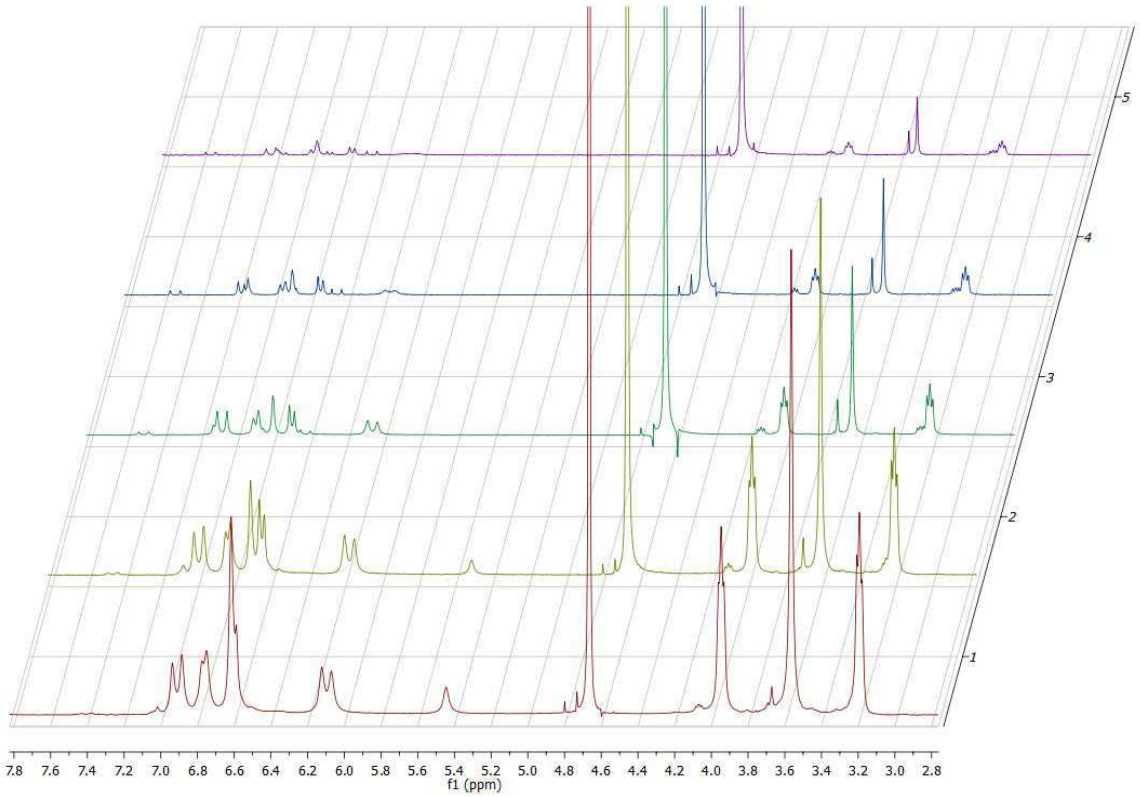


**Figure 6:** Proton NMR spectra of (**4**) in concentration of 20 mM (1), 10 mM (2), 5 mM (3), 2 mM (4), 1 mM (5) in $D_2O$; x-values (f1) in ppm relative to external standard TMS, 1 ppm = 400 Hz.

The NMR spectra of **4** shows an initial aggregation between 1 and 2 mM by shift of the signals and change in their multiplet structure in the aromatic region (6.5 – 8 ppm). This observation is confirmed with compound **8** (see supporting information for spectra). Therefore, aggregation phenomena in aqueous media can be neglected below 1 mM. No influence on results of the biological studies covered here is expected. Typical therapeutic concentrations in aPDT are in the micromolar range (5 to 250 µM).

The molecules´ pH stability was determined by recording UV-Vis spectra of compounds **4** and **8** in buffer solutions at different pH values following incubation for 4 hours. The novel derivatives showed excellent stability in acidic medium (down to pH = 2), but decompose slowly in alkaline solutions with pH >10 (see supporting information for spectra).

Below pH 7, the parent compound curcumin (**1**) is stabilized but parallel with the decreasing pH values, the dissociation equilibrium shifts towards the neutral form of very low aqueous solubility. [63] Lowering solubility in acidic conditions is not possible in the novel derivatives, as the phenolic OH group was substituted. Neither a precipitate at lower pH nor a spectral change was observed with **4** at pH 2. Thus the spectral characteristics of the novel photosensitizers are kept constant over a wider range which is known from curcumin so far.[64, 65] A change of the spectrum occurs first at pH > 8.

The temperature stability was exemplarily investigated with compound **4** by temperature dependent NMR studies in DMSO-d6 and $D_2O$. Figure 7 shows the data collected for compound **4** in 10°C steps. No change appeared in the spectrum after heating to 130 °C for more than 10 minutes. The compounds are therefore temperature stable in solution under typical therapeutic conditions:

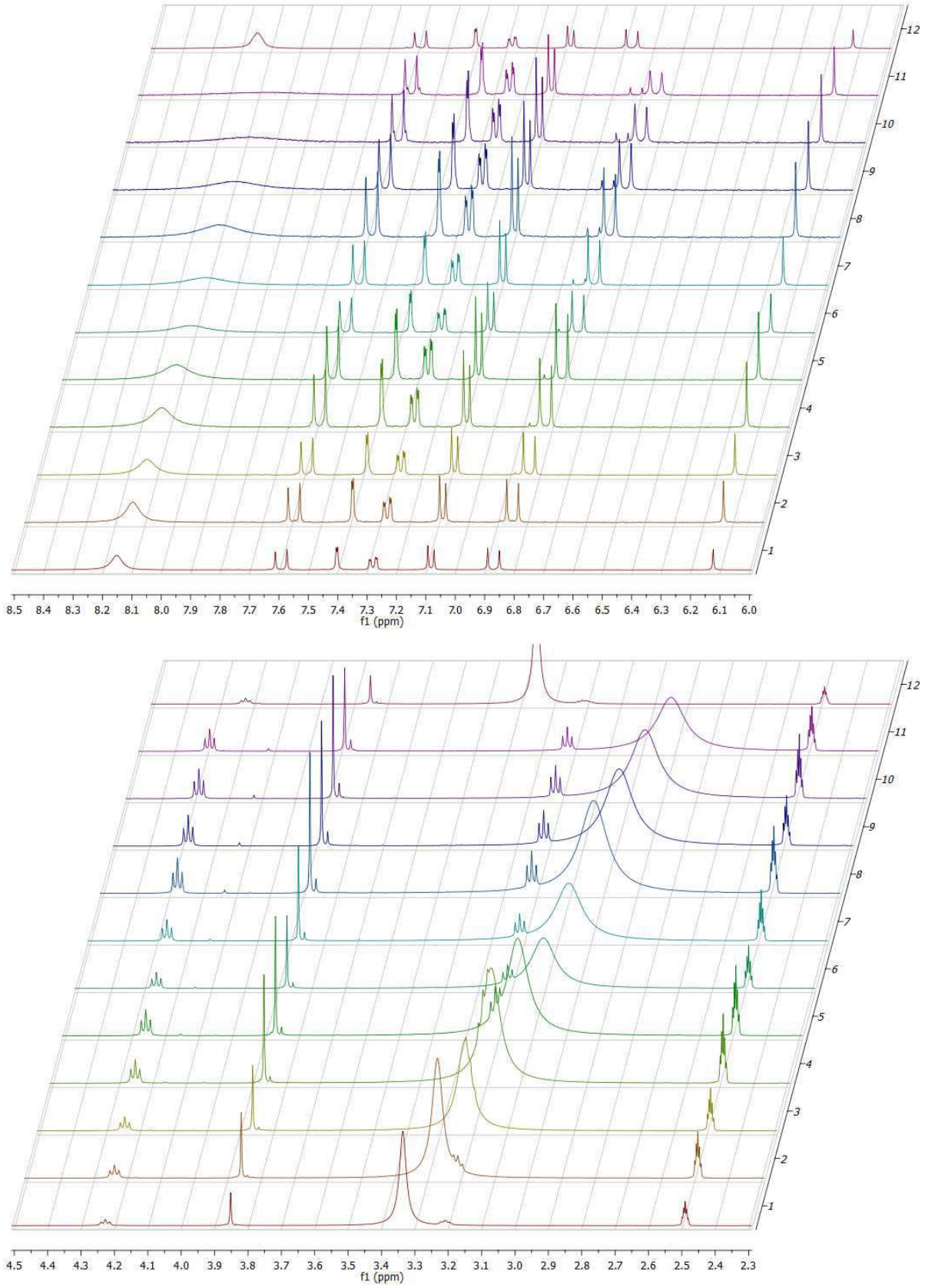


**Figure 7:** Temperature stability of **4** by NMR in DMSO-d6; temperature steps: room temperature (1), 40 °C (2), 50 °C (3),60 °C (4), 70 °C (5), 80 °C (6), 90 °C (7), 100 °C (8),

110 °C (9), 120 °C (10)and 130 °C (11), then cooling to room temperature (12), c = 10 mM; x-values (f1) in ppm relative to external standard TMS, 1 ppm = 400 Hz.

Again the shift of the spectrum in the aromatic region of approx. 0.1 ppm indicates aggregation in the millimolar range (c = 10 mM).

Our results suggest that the attachment of the cationic substituents to the phenolic OH moiety significantly stabilizes the chromophore against temperature influences in solution as well as alkaline pH values.

**Photodynamic Inactivation of Bacteria (PDI):**

Prime candidates for this study are compound **2**, compound **4** ("SACUR-1"), compound **7** ("SACUR-2") and compound **8** ("SACUR-3"). Photodynamic Inactivation was performed against bacteria in suspension using different concentrations of each derivative (10 µM, 25 µM and 50 µM). All curcumin derivatives were evaluated against Gram(-) *E. coli* (LED light source with $\lambda_{max,em}$= 435 nm and 9.4 mW/cm²) as these are known to be more difficult targets for antibacterial therapies when compared to Gram(+) species (table 2). In succession two derivatives (**4**, **8**) were also tested against Gram(+) *S. aureus* in comparison to Gram(-) *E. coli* using shorter exposure periods with a more powerful light source (BlueV, $\lambda_{em}$= 390 - 460 nm 17.5 mW/cm²) (fig. 3).

To exclude a contribution of photodegradation products to the toxicity of the compounds we mixed bacteria with a pre-illuminated sample of 10 µM solution of compound **4**. No decrease in the number of viable bacteria was observed after incubation with *E. coli* in the dark (data not shown).

A bacterial cytotoxicity of the excitation light ($\lambda_{max,em}$= 435 nm, 33.8 J / cm²) was never observed (figure 8, "LO"). Prior to light exposure bacteria samples were washed with buffer

medium once. The efficiency of PDI is not dependent on the washing step (confirmed by control experiments with **8**) (data not shown).

As curcumin-derived compounds have pan-assay interference compounds (PAINS) substructures that have the potential to cause misleading results, we carefully conducted controls. Without light no effect was observed on the viability of the bacterial cells (Fig.8 & Fig.9). [66] Light alone hat also no effect. Antimicrobial activity of the curcumin derivatives only became apparent after illumination. Therefore, no disturbance of our assay is assumed.

Compound **4** is the direct analog to natural curcumin (figure 1) and therefore is of special interest. It can be easily produced starting from natural curcumin (scheme 3). Incubation with 50 µM **4** induced >3 $\log_{10}$ reduction of the CFU counts upon 5 min of incubation. Contrary to the use of 10 µM, a longer incubation period with 50 µM did result in antibacterial effect of ~ 6 $\log_{10}$ reduction upon 25 min incubation.

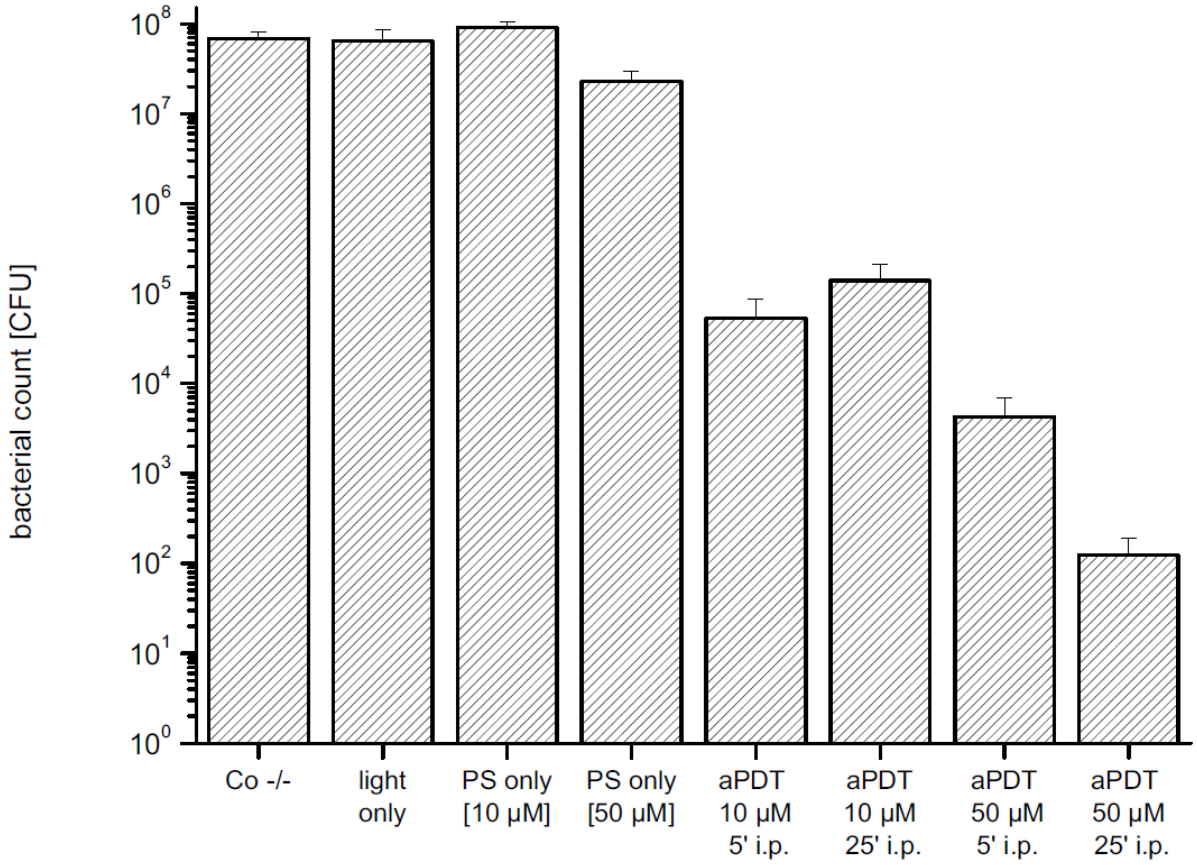

**Figure 8:** Phototoxicity of **4** towards *E. coli* (435 nm LED-illumination, 33.8 J/cm$^2$). Colonies were counted 24 h post illumination. Bars represent the median of the absolute CFU count of three independent biological replicates. Error bars show the standard deviation. Co -/-: double negative control, PS only: photosensitizer only without illumination, i.p. indicates the incubation time with the photosensitizer. PDI: Photodynamic inactivation. LO: light only control did not result in a change in bacterial count, not shown.

At 50 µM of **4**, a low dark toxicity (~0.5 log) was observed, which is within the error margins of the experiment. Presumably efficiency can be increased by optimizing the light source (see figure 8) and illumination time.

Compound **8** contains in comparison to **4** two additional amine hydrochloride substituents, thus carrying four positive charges (figure 1). After incubation with 10 µM of **8** for either 5 or 25 min a reduction of viable *E. coli* below detection limit was observed after illumination (> 7 $\log_{10}$ reduction). The number of viable bacterial cells decreased about 1 $\log_{10}$ without illumination subsequent to incubation with at 50 µM. Photosensitizer **8** was identified as the most effective one investigated in this study (figure 9).

Thus, for **8** three lower concentrations (1µM, 5µM and 7.5µM) were tested (figure 9 A). The minimal concentration to reach a reduction of 3$\log_{10}$ (99.9%) for for successful PDI was 5 µM. At a concentration of 10 µM still approx. 5 $\log_{10}$ of inactivation was observed (figure 9 B). With 10µM of **8** no cytotoxicity without light exposure is found (figure 9 A).

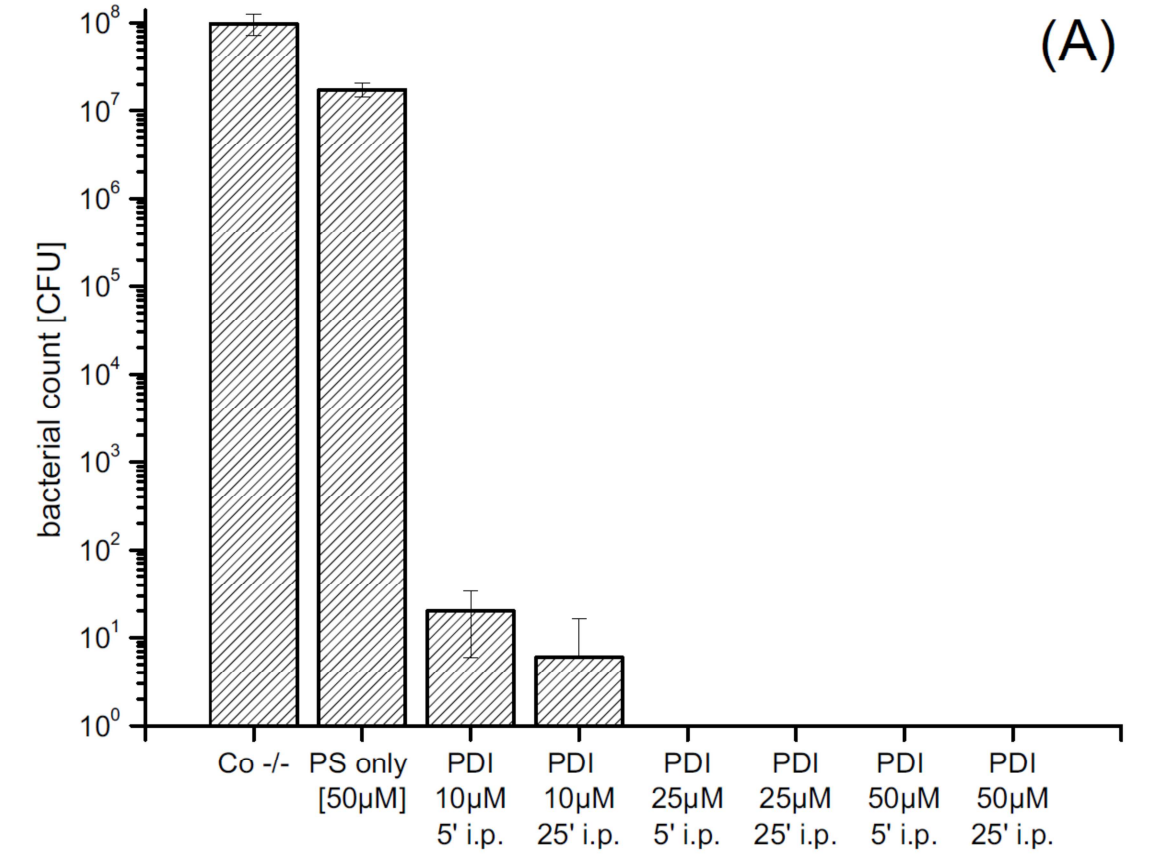
(A)
bacterial count [CFU]
$10^8$
$10^7$
$10^6$
$10^5$
$10^4$
$10^3$
$10^2$
$10^1$
$10^0$
Co -/-
PS only [50μM]
PDI 10μM 5' i.p.
PDI 10μM 25' i.p.
PDI 25μM 5' i.p.
PDI 25μM 25' i.p.
PDI 50μM 5' i.p.
PDI 50μM 25' i.p.

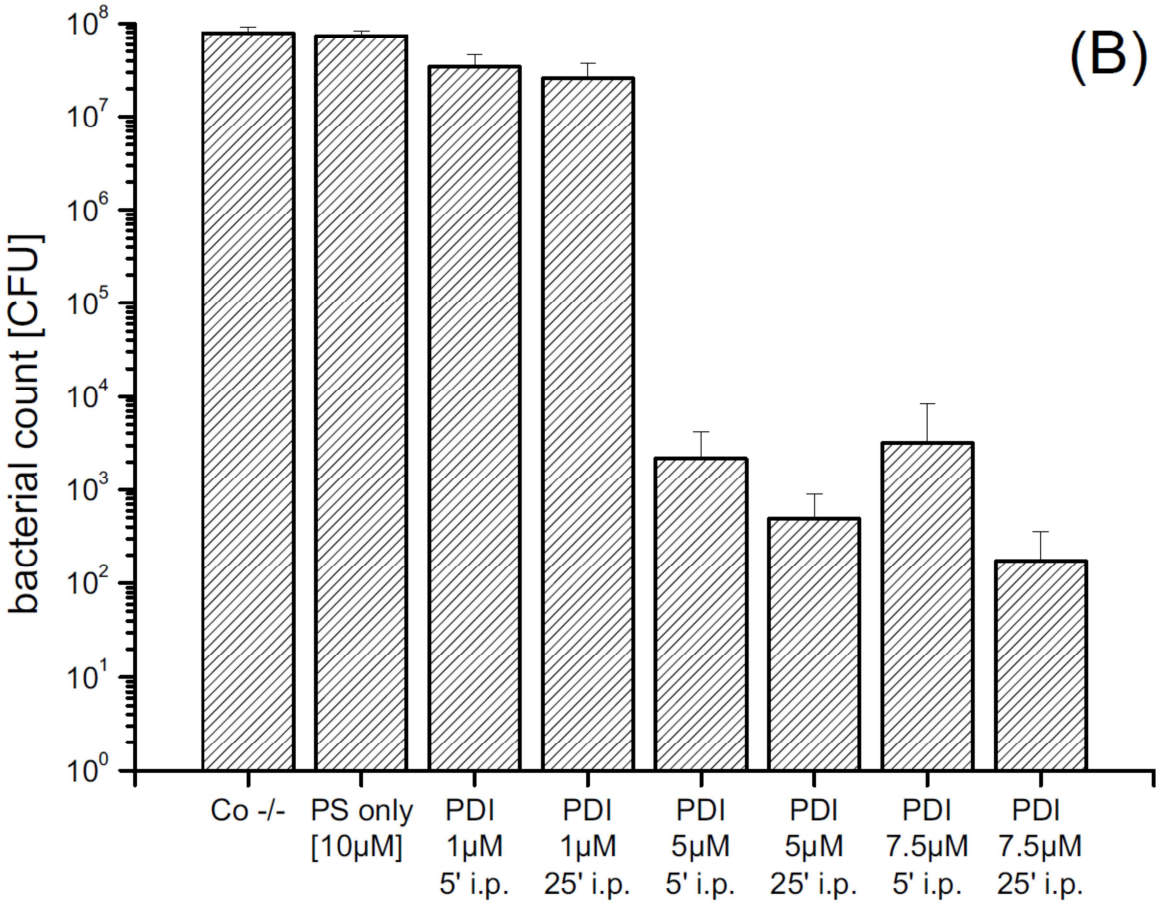
(B)
bacterial count [CFU]
$10^8$
$10^7$
$10^6$
$10^5$
$10^4$
$10^3$
$10^2$
$10^1$
$10^0$
Co -/-
PS only [10μM]
PDI 1μM 5' i.p.
PDI 1μM 25' i.p.
PDI 5μM 5' i.p.
PDI 5μM 25' i.p.
PDI 7.5μM 5' i.p.
PDI 7.5μM 25' i.p.

**Figure 9:** Phototoxicity of **8** towards *E. coli* (435 nm LED-illumination with 33.8 J/cm$^2$). The subplot (B) shows the absolute CFU count for 10-50 µM concentration, the subplot (A) 1-7.5 µM. Colonies were counted 24 h post illumination. Bars represent the relative inactivation gained from the average of three independent biological replicates. Error bars show the standard deviation. Co -/-: double negative control, PS only: photosensitizer only without illumination, i.p. indicates the incubation time with the photosensitizer. PDI: Photodynamic inactivation.

Even quite short illumination periods are sufficient for an effective PDI: at a fixed concentration of 10 µM of **8 a**n antimicrobial effect (99.9 % killing; 3 $\log_{10}$) can be achieved after 1.5 minutes (dose of ~ 0.85 J/cm$^2$), more than 5 $\log_{10}$ reduction of viable *E. coli* was found after only 2.5 minutes of illumination corresponding to a dose of 1.41 J/cm$^2$ (data not shown).

The remaining compounds were screened vs. *E. coli*, to estimate the impact of the structural differences on the efficacy for bacterial inactivation (table 2).

Compound **2** is the smallest molecule in the series without any additional functionalization and depicts the basic structure all other curcuminoids are derived from. Essentially it is bisdemethoxycurcumin (one of the natural occurring curcuminoids) with the hydroxyl groups replaced by aminoethoxyhydrochloride (figure 1). Incubation with 50 µM of **2** for 25 min induced more than 7 $\log_{10}$ reduction (table 2).

In **5** the methoxy substituents are at a different position of the phenyl rings than in **4**. The strong correlation with the photodynamic effect due both incubation period and is noticeable. Remarkably, incubation with 50 µM **4** for 25 min induced a reduction of viable *E. coli* below the detection limit. Compound **7** features a more hydrophilic ethylene glycol spacer between the cationic charged moiety and the curcumin chromophor. This change increases polarity, resulting in a slightly higher efficacy in comparison to **4**, but is not resulting in higher killing

rates than observed for **2**. Reduction of the bacterial count below detection limit was reached upon 25 min incubation with 50 µM **7**.

Compound **3** carries an extra methyl groups as second substituent at the phenyl ring replacing the methoxy group of the curcumin analog **4**. The resulting photodynamic effect was slightly stronger than with **2**. After five minute incubation more than 6 $\log_{10}$ reduction was reached, with a comparatively large variation. Incubation with 50 µM **3** for 25 min induced a reduction of viable *E. coli* below detection limit (table 2).

In **6** two benzyloxy substituents were added to the molecule in order to increase the lipophilicity further. Photodynamic Inactivation using **6** resulted in a comparatively large variation in the decrease of viable *E. coli* bacteria inducing close to 5 orders of magnitude inactivation using optimized parameters. Therefore **6** was the least effective compound in this study. The substitution causes a doubling in molecular weight. This may prevent accessibility to the cell membrane by limited transition through the bacterial cell wall.

The highest efficacy of compound **8** in comparison to all others is reasoned by two additional hydrochlorides. The two resulting additional cations might govern better cell attachment. Interestingly, there is no rise in antimicrobial efficacy if the compound is equipped with two more hydrochlorides, thus further increasing the charge number to six in structure **9**. This compound exhibits an antimicrobial effect comparable with **2**. Upon incubation with 50 µM **9** less than 10 *E. coli* in per 100 µL were able to form colonies (>7 $\log_{10}$ reduction). No influence of the incubation period became apparent (table 2).

The order of efficacy correlated with the number of cationic charges, applicable to other photosensitizers could be verified only for the bi- and tetra- substituted compounds.

Table 2 shows the effect of the curcumin derivatives (**2** – **9**) against *E. coli* (ATCC25922) using the 435nm LED light source (38 mJ/ cm²). The averaged reference control (no light, no PS) was $10^8$/mL.

| Compound | | reduction CFU in $log_{10}$ | | | |
|---|---|---|---|---|---|
| | | 5 min incubation | | 25 min incubation | |
| | | 10 µM | 50 µM | 10 µM | 50 µM |
| Compound **2** | | > 4 | > 6 | > 5 | > 6 |
| Compound **3** | | > 5 | > 4 | > 5 | > 7 |
| Compound **4** | ***SACUR-1*** | > 1 | > 5 | >2 | > 5 |
| Compound **5** | | > 2 | > 5 | > 3 | > 7 |
| Compound **6** | | > 1 | > 3 | > 3 | > 4 |
| Compound **7** | ***SACUR-2*** | > 2 | > 6 | > 4 | > 7 |
| Compound **8** | ***SACUR-3*** | >6 | > 7 | >6 | > 7 |
| Compound **9** | | > 4 | > 7 | > 4 | > 7 |

**Table 2:** Photodynamic inactivation rates of all compounds (**2** – **9**) against *E. coli* upon light activation (33.8 J/cm$^2$).[a] Shown is the logarithmic decay after exposure with respect to the reference control: - indicates < 1 $log_{10}$ step reduction of CFU, which was defined as virtually no antibacterial photodynamic efficacy. Thresholds for evaluation of antibacterial efficacy were inactivation rates of ≥ 3 $log_{10}$ steps (99.9%; antibacterial effect, light grey) and ≥ 5 $log_{10}$ steps (99.999%; disinfectant effect, dark grey).

A figure (S-38) showing the results of the single parameters combined for each curcuminoid and sorted in rising efficacy is shown in the supporting information.

The antimicrobial photodynamic efficacy of compound **4** and **8** was investigated in more detail using shorter illumination times and lower energy doses. For use under practical clinical parameters a light source with an improved overlap to the spectrum of the compounds was employed (clinical therapy lamp BlueV, Waldman GmbH, see figure 3). The aim was to evaluate (a) if **4** shows higher efficacy using an more optimal light source and (b) to figure out

the scope and limitations of the most effective compound **8** against Gram(+) *S. aureus* as a model organism for MRSA.

With the BlueV lamp for *E. coli* a light dose of 15.7 J /cm² (15 min exposure) and for *S. aureus* a light dose of 5.3 J /cm² (5 min. exposure) was applied. Table 3 summarizes the results. The averaged reference control (no light, no PS) is for *E. coli* $3.6x10^8$/mL and for *S. aureus* $3.9x10^8$/mL.

| Compound | | reduction CFU in $log_{10}$ | | | |
|---|---|---|---|---|---|
| | | *E. coli* | | *S. aureus* | |
| | | 10 µM | 50 µM | 10 µM | 50 µM |
| Compound **4** | ***SACUR-1*** | > 4 | > 5 | > 3 | > 5 |
| Compound **8** | ***SACUR-3*** | > 4 | > 5 | > 4 | > 5 |

**Table 3:** Photodynamic inactivation rates of compounds **4** and **8** against *E. coli* and *S. aureus* upon light activation (BlueV light source). Incubation time was 1 min. Shown is the logarithmic decay after exposure with respect to the reference control. Thresholds for evaluation of antibacterial efficacy were inactivation rates of ≥ 3 $log_{10}$ steps (99.9%; antibacterial effect, light gray) and ≥ 5 $log_{10}$ steps (99.999%; disinfectant effect, dark grey).

Upon illumination with the BlueV light source an antibacterial effect equals disinfection (> 5 $log_{10}$ reduction) can be realized in minutes with the novel derivatives applying light dose of 15.7J /cm² for *E. coli* and only 5.3J /cm² for *S. aureus*.

As shown in the figures 9 and 10, an illumination of the bacterial strains *S. aureus* and *E. coli* with doses of blue light as described above (BlueV light source: 390 - 460nm or LED light source: 435 nm) in the absence of a photosensitizer (0µM of the respective curcumin) did not affect the number of surviving microorganisms as compared to the unexposed control.

With all curcuminoids investigated in this study at least a >3 $log_{10}$ reduction was achieved upon 25 min incubation with 50 µM photosensitizer (see figure 9 and supplementary information). 3 $log_{10}$ equates a reduction of 99.9 % in bacterial count and is, according to the American Society of Microbiology, the criterion for an antimicrobial effect. In comparison to the efficacy of PVP curcumin [67] the novel derivatives showed substantially improved

efficacy. If using 50 µM PVP complexed curcumin (PVP-CUR) no reduction was observed and only 0.3 $\log_{10}$ of bacteria were killed with100 µM PVP-CUR.

The improvement of all tested curcuminoids can be traced back to a hydrochloride connected via an ethoxy group (aminoethoxyhydrochloride) to the phenyl ring. The salt further enhances water-solubility [67] and the cation of the salt is expected to facilitate interaction with the cell wall. A direct comparison of photosensitizers is multi-factorial. For illumination, bacterial counting and incubation no consistent procedure and equipment exists among research groups so far. At least within this study consistent conditions should be provided. Furthermore to be more precise, the observed effect should be normalized to the number of photons absorbed by the individual photosensitizer. [68] This can be calculated by the sum of photons absorbed at each emission wavelength of the illumination source. This was not performed due to the fact that absorption spectra (figure 2) of most curcuminoids presented in this study show comparable absorption values at 435 nm Still, spectra of **2** and **9** deviate slightly upwards in strength of absorption. To compensate for this deviation a reduction of applied light energy could be a solution. In contrast, the spectrum of **5** absorbs less at 435 nm and would require a raise in light fluence. Nonetheless, with exception for **5** the impact of a little change in light fluence is not expected to be significant. In order to avoid differences due to a different extend of light absorption, light was applied in excess. The illumination period needs to be optimized for each photosensitizer and application separately in further investigations. For **5** comparability remains arguable. However, the observed photodynamic effect (reduction of viable *E. coli* below detection limit, 25 min i.p.; 50 µM) shows that light absorption was sufficient and it is a debatable point whether much higher light fluence application is practicable. Light exposure can also lead to photobleaching of the photosensitizer. If there would be a wavelength shift in absorption shifting the absorption spectrum out of the emission spectrum, the light source would have to be adapted. Yet, in the range from 350 nm

to 600 nm neither a significant shift nor another peak was observed for **5** (see figure 2). In practice it should be considered that for excitation of **5** a higher light fluence might be needed than for the other tested curcuminoids.

The comparison of the curcuminoids was done in equal liquid suspensions. Different chemical and physical conditions might have an impact on the photoefficacy due to interactions with the molecular environment. Therefore, each of the compounds tested might be the best choice for a specific application. However, for all synthesized curcuminoids it should be kept in mind that the bioavailibity might differ from the naturally occurring curcuminoids.

## Conclusion:

Curcumin derived from rhizome of turmeric is composed of three different curcuminoids. If not supersaturated [69] or applied in formulations with other constituents,[67] none of these show a phototoxic effect towards *E. coli*. The aim of this study was the investigation of the properties of novel cationic curcumin derivatives with focus on comparisons of the efficacy of these photosensitizers towards *E. coli.* Eight newly synthesized photosensitizers were tested and compared to each other. With this structure-activity relationship study the influence of different substituents to photodynamic inactivation was demonstrated. A less polar substituent seems to cause a decrease in effectiveness against *E. coli*, whereas high hydrophilicity and four positive charges seem to be advantageous for antimicrobial action against Gram-negatives. A suboptimal balance between charge and lipophilicity can be an explanation for a weaker and / or slower attachment to the cell wall.

The light activation of the new curcumin derivatives **2** to **9** achieved antibacterial efficacy against the key pathogens of 99.999% (*S. aureus*) or even 99.9999 % (*E. coli*) at concentrations of at least 5 µM of the respective PS.

All derivatives showed high stability over a wide range of changing pH (2 – 10), good temperature-stability and photostability in the therapeutic time window for typical aPDT applications. This was accompanied by successful development of a straight forward and simplified synthesis and purification protocol for the novel compounds. The high selectivity and the excellent yields of the Mitsonubo reaction with natural curcumin opened a way to quick and simple modification of the natural molecule.

Particularly with regard to the progressing ineffectiveness of antibiotics towards multi drug resistant bacteria, photodynamic inactivation of microbial pathogens is a powerful tool with a broad application spectrum and no major side effects. All compounds, with **8** being of outstanding efficacy, were identified being able to promote photodynamic inactivation as alternative to or in combination with other antimicrobial approaches. The novel photosensitizers based on curcumin presented allow for effective eradication of *E. coli* without the need for addition of permeabilizing agents. Photodynamic Inactivation using these compounds against Gram(+) and Gram(-) pathogens therefore may be a realistic prospect for future clinical use. They may display an alternative to antibiotics and are of special interest due to the fact, that Gram(-) bacteria like *E. coli* display a lower accessibility by curcumin than Gram(+). [62]

The potential of natural curcumin as photosensitizer is limited by its low aqueous solubility, susceptibility to hydrolytic and photolytic degradation, and low accessibility to Gram(-) bacteria. The new curcumin derivatives were successfully designed to overcome these problems.

Ongoing studies in our lab extending our investigations into this interesting molecule class towards other key pathogens while also investigating a library of substitution patterns, will show the scope and limitations of a pure Type I sensitizer for antimicrobial photodynamic therapy. The application to foodstuff needs further investigation to estimate whether aPDT

with curcumin derivatives is an alternative to conventional disinfection methods. They may offer excellent efficacy under oxygen poor conditions and may also act as effective agents for anti-biofilm applications, especially in a hypoxic environment.

## Acknowledgement

Martin Rappl, Tobias Graf and Dipl.-Phys. Michael Glueck are gratefully acknowledged for excellent technical assistance. Anita Gollmer is acknowledged for measurement of singlet oxygen quantum yields. All authors declare that they have no conflict of interest. We would like to thank Dr. Manfred Binder for proof reading of the manuscript.

## Abbreviations

Staphylococcus aureus (SA) and Escherichia coli (EC), antimicrobial photodynamic therapy (aPDT), colony forming unit (CFU), incubation time (i.p.), light only control (LO), reactive oxygen species (ROS), nuclear magnetic resonance (NMR), high performance liquid chromatography (HPLC), mass spectroscopy (MS), curcumin (CUC), polyvinylpyrrolidon (PVP), Extended-Spectrum-Betalaktamase (ESBL), dimethylsulfoxide (DMSO), Dulbecco`s Phosphate Buffered Saline (DPBS), enterohemorrhagic E. coli (EHEC), relative centrifugal force (rcf), rounds per minute (rpm), world health organization (WHO)

## Associated Content

For experimental details, materials and methods relating to synthesis and characterization, selected NMR spectra, UV-Vis data concerning aggregation and stability please see the **Supporting Information**.

## References

[1] J. O'Neill, R. Minghui, N. Kuo, S. Chaudhry, M.W. Bonney, S. Solomon, J.K. Hamied, M.O. Moraes, E. Goosby, TACKLING DRUG-RESISTANT INFECTIONS GLOBALLY: FINAL REPORT AND RECOMMENDATIONS, https://amr-review.org/, (2016).

[2] R. Wise, Antimicrobial resistance: priorities for action, J Antimicrob Chemother, 49 (2002) 585-586.

[3] A.R. Coates, G. Halls, Y. Hu, Novel classes of antibiotics or more of the same?, Br J Pharmacol, 163 (2011) 184-194.

[4] WHO, Antimicrobial resistance. Global report on surveillance, http://apps.who.int/iris/bitstream/10665/112642/1/9789241564748_eng.pdf?ua=1, (2014).

[5] C.f.D.C.a. Prevention, Antibiotic resistance threats in the United States, http://www.cdc.gov/drugresistance/pdf/ar-threats-2013-508.pdf, (2013).

[6] T. Guardian, UN meeting tackles the 'fundamental threat' of antibiotic-resistant superbugs in, https://www.theguardian.com/society/2016/sep/20/un-declaration-antibiotic-drug-resistance, 2016.

[7] B.D. Schindler, P. Jacinto, G.W. Kaatz, Inhibition of drug efflux pumps in Staphylococcus aureus: current status of potentiating existing antibiotics, Future Microbiol, 8 (2013) 491-507.

[8] L. Kalan, G.D. Wright, Antibiotic adjuvants: multicomponent anti-infective strategies, Expert Rev Mol Med, 13 (2011) e5.

[9] S.K. Rod, F. Hansen, F. Leipold, S. Knochel, Cold atmospheric pressure plasma treatment of ready-to-eat meat: inactivation of Listeria innocua and changes in product quality, Food Microbiol, 30 (2012) 233-238.

[10] M.B. Oleksiewicz, G. Nagy, E. Nagy, Anti-bacterial monoclonal antibodies: back to the future?, Arch Biochem Biophys, 526 (2012) 124-131.

[11] S.T. Abedon, S.J. Kuhl, B.G. Blasdel, E.M. Kutter, Phage treatment of human infections, Bacteriophage, 1 (2011) 66-85.

[12] E. Alves, M.A. Faustino, M.G. Neves, A. Cunha, J. Tome, A. Almeida, An insight on bacterial cellular targets of photodynamic inactivation, Future Med Chem, 6 (2014) 141-164.

[13] T. Dai, Y.Y. Huang, M.R. Hamblin, Photodynamic therapy for localized infections--state of the art, Photodiagnosis Photodyn Ther, 6 (2009) 170-188.

[14] H.P. Ammon, M.A. Wahl, Pharmacology of Curcuma longa, Planta Med, 57 (1991) 1-7.

[15] N. Chainani-Wu, Safety and anti-inflammatory activity of curcumin: a component of tumeric (Curcuma longa), J Altern Complement Med, 9 (2003) 161-168.

[16] H. Zhu, T. Xu, C. Qiu, B. Wu, Y. Zhang, L. Chen, Q. Xia, C. Li, B. Zhou, Z. Liu, G. Liang, Synthesis and optimization of novel allylated mono-carbonyl analogs of curcumin (MACs) act as potent anti-inflammatory agents against LPS-induced acute lung injury (ALI) in rats, Eur J Med Chem, 121 (2016) 181-193.

[17] A. Noorafshan, S. Ashkani-Esfahani, A review of therapeutic effects of curcumin, Curr Pharm Des, 19 (2013) 2032-2046.

[18] P.K. Sahu, Design, structure activity relationship, cytotoxicity and evaluation of antioxidant activity of curcumin derivatives/analogues, Eur J Med Chem, 121 (2016) 510-516.

[19] T.A. Nguyen, A.J. Friedman, Curcumin: a novel treatment for skin-related disorders, J Drugs Dermatol, 12 (2013) 1131-1137.

[20] B. Chandran, A. Goel, A randomized, pilot study to assess the efficacy and safety of curcumin in patients with active rheumatoid arthritis, Phytother Res, 26 (2012) 1719-1725.

[21] S.D. Deodhar, R. Sethi, R.C. Srimal, Preliminary study on antirheumatic activity of curcumin (diferuloyl methane), Indian J Med Res, 71 (1980) 632-634.

[22] T. Dorai, J. Diouri, O. O'Shea, S.B. Doty, Curcumin Inhibits Prostate Cancer Bone Metastasis by Up-Regulating Bone Morphogenic Protein-7 in Vivo, J Cancer Ther, 5 (2014) 369-386.

[23] P.M. Luthra, N. Lal, Prospective of curcumin, a pleiotropic signalling molecule from Curcuma longa in the treatment of Glioblastoma, Eur J Med Chem, 109 (2016) 23-35.

[24] A.B. Kunnumakkara, P. Anand, B.B. Aggarwal, Curcumin inhibits proliferation, invasion, angiogenesis and metastasis of different cancers through interaction with multiple cell signaling proteins, Cancer Lett, 269 (2008) 199-225.

[25] T. Ahmed, A.H. Gilani, Therapeutic potential of turmeric in Alzheimer's disease: curcumin or curcuminoids?, Phytother Res, 28 (2014) 517-525.

[26] J.S. Jurenka, Anti-inflammatory properties of curcumin, a major constituent of Curcuma longa: a review of preclinical and clinical research, Altern Med Rev, 14 (2009) 141-153.

[27] A. Barzegar, The role of electron-transfer and H-atom donation on the superb antioxidant activity and free radical reaction of curcumin, Food Chem, 135 (2012) 1369-1376.

[28] A. Barzegar, A.A. Moosavi-Movahedi, Intracellular ROS protection efficiency and free radical-scavenging activity of curcumin, PLoS One, 6 (2011) e26012.

[29] J.K. Lin, S.Y. Lin-Shiau, Mechanisms of cancer chemoprevention by curcumin, Proc Natl Sci Counc Repub China B, 25 (2001) 59-66.

[30] G.Y. Liu, Y.Z. Sun, N. Zhou, X.M. Du, J. Yang, S.J. Guo, 3,3'-OH curcumin causes apoptosis in HepG2 cells through ROS-mediated pathway, Eur J Med Chem, 112 (2016) 157-163.

[31] S. Kumar, U. Narain, S. Tripathi, K. Misra, Syntheses of Curcumin Bioconjugates and Study of Their Antibacterial Activities against beta-Lactamase-Producing Microorganisms, Bioconjug Chem, 12 (2001) 464-469.

[32] T. Haukvik, E. Bruzell, S. Kristensen, H.H. Tonnesen, A screening of curcumin derivatives for antibacterial phototoxic effects studies on curcumin and curcuminoids. XLIII, Pharmazie, 66 (2011) 69-74.

[33] M. Heger, R.F. van Golen, M. Broekgaarden, M.C. Michel, The molecular basis for the pharmacokinetics and pharmacodynamics of curcumin and its metabolites in relation to cancer, Pharmacol Rev, 66 (2014) 222-307.

[34] Y.H. An, R.J. Friedman, Concise review of mechanisms of bacterial adhesion to biomaterial surfaces, J Biomed Mater Res, 43 (1998) 338-348.

[35] B. Bukau, J.M. Brass, W. Boos, Ca2+-induced permeabilization of the Escherichia coli outer membrane: comparison of transformation and reconstitution of binding-protein-dependent transport, J Bacteriol, 163 (1985) 61-68.

[36] T. Maisch, J. Wagner, V. Papastamou, H.J. Nerl, K.A. Hiller, R.M. Szeimies, G. Schmalz, Combination of 10% EDTA, Photosan, and a blue light hand-held photopolymerizer to inactivate leading oral bacteria in dentistry in vitro, J Appl Microbiol, 107 (2009) 1569-1578.

[37] H.H. Tonnesen, J. Karlsen, G.B. van Henegouwen, Studies on curcumin and curcuminoids. VIII. Photochemical stability of curcumin, Z Lebensm Unters Forsch, 183 (1986) 116-122.

[38] A. Kunwar, A. Barik, S.K. Sandur, K. Indira Priyadarsini, Differential antioxidant/pro-oxidant activity of dimethoxycurcumin, a synthetic analogue of curcumin, Free Radic Res, 45 (2011) 959-965.

[39] J. Trujillo, Y.I. Chirino, E. Molina-Jijon, A.C. Anderica-Romero, E. Tapia, J. Pedraza-Chaverri, Renoprotective effect of the antioxidant curcumin: Recent findings, Redox Biol, 1 (2013) 448-456.

[40] A. Felgentrager, T. Maisch, D. Dobler, A. Spath, Hydrogen bond acceptors and additional cationic charges in methylene blue derivatives: photophysics and antimicrobial efficiency, Biomed Res Int, 2013 (2013) 482167.

[41] J.C. Miller, M.O. Mitchell, Method for the synthesis of curcumin analogues, in, USA, 2009.

[42] O. Mitsunobu, Y. Yamada, Preparation of Esters of Carboxylic and Phosphoric Acid via Quarternary Phosphonium Salts, Bull. Chem. Soc. Japan, 40 (1967) 2380-2382.

[43] A. Barik, K. Indira Priyadarsini, Solvent dependent photophysical properties of dimethoxy curcumin, Spectrochim Acta A Mol Biomol Spectrosc, 105 (2013) 267-272.

[44] J. Baier, T. Maisch, J. Regensburger, M. Loibl, R. Vasold, W. Baumler, Time dependence of singlet oxygen luminescence provides an indication of oxygen concentration during oxygen consumption, J Biomed Opt, 12 (2007) 064008.

[45] W. Baumler, J. Regensburger, A. Knak, A. Felgentrager, T. Maisch, UVA and endogenous photosensitizers--the detection of singlet oxygen by its luminescence, Photochem Photobiol Sci, 11 (2012) 107-117.

[46] J. Regensburger, T. Maisch, A. Knak, A. Gollmer, A. Felgentraeger, K. Lehner, W. Baeumler, UVA irradiation of fatty acids and their oxidized products substantially increases their ability to generate singlet oxygen, Phys Chem Chem Phys, 15 (2013) 17672-17680.

[47] A. Gollmer, J. Regensburger, T. Maisch, W. Baumler, Luminescence spectroscopy of singlet oxygen enables monitoring of oxygen consumption in biological systems consisting of fatty acids, Phys Chem Chem Phys, 15 (2013) 11386-11393.

[48] A.A. Miles, S.S. Misra, J.O. Irwin, The estimation of the bactericidal power of the blood, J Hyg (Lond), 38 (1938) 732-749.

[49] A. Kunwar, S.K. Sandur, M. Krishna, K.I. Priyadarsini, Curcumin mediates time and concentration dependent regulation of redox homeostasis leading to cytotoxicity in macrophage cells, Eur J Pharmacol, 611 (2009) 8-16.

[50] Y. Manolova, V. Deneva, L. Antonov, E. Drakalska, D. Momekova, N. Lambov, The effect of the water on the curcumin tautomerism: a quantitative approach, Spectrochim Acta A Mol Biomol Spectrosc, 132 (2014) 815-820.

[51] L. Nardo, A. Andreoni, M. Bondani, M. Masson, T. Haukvik, H.H. Tonnesen, Studies on curcumin and curcuminoids. XLVI. Photophysical properties of dimethoxycurcumin and bis-dehydroxycurcumin, J Fluoresc, 22 (2012) 597-608.

[52] L. Nardo, A. Maspero, M. Selva, M. Bondani, G. Palmisano, E. Ferrari, M. Saladini, Excited-state dynamics of bis-dehydroxycurcumin carboxylic acid, a water-soluble derivative of the photosensitizer curcumin, J Phys Chem A, 116 (2012) 9321-9330.

[53] L.G. Arnaut, M.M. Pereira, J.M. Dabrowski, E.F. Silva, F.A. Schaberle, A.R. Abreu, L.B. Rocha, M.M. Barsan, K. Urbanska, G. Stochel, C.M. Brett, Photodynamic therapy efficacy enhanced by dynamics: the role of charge transfer and photostability in the selection of photosensitizers, Chemistry, 20 (2014) 5346-5357.

[54] P. Galer, A. Golobic, J. Koller, B. Kosmrlj, B. Sket, Structures in solid state and solution of dimethoxy curcuminoids: regioselective bromination and chlorination, Chem Cent J, 7 (2013) 107.

[55] Y.J. Wang, M.H. Pan, A.L. Cheng, L.I. Lin, Y.S. Ho, C.Y. Hsieh, J.K. Lin, Stability of curcumin in buffer solutions and characterization of its degradation products, J Pharm Biomed Anal, 15 (1997) 1867-1876.

[56] F. Gueraud, M. Atalay, N. Bresgen, A. Cipak, P.M. Eckl, L. Huc, I. Jouanin, W. Siems, K. Uchida, Chemistry and biochemistry of lipid peroxidation products, Free Radic Res, 44 (2010) 1098-1124.

[57] C. Schneider, A. Amberg, J. Feurle, A. Ro, M. Roth, G. Toth, P. Schreier, 2-[4'-Hydroxy-3'-methoxy)-phenoxy]-4-(4''-hydroxy-3''-methoxy-phenyl)-8-hydroxy-6-oxo-3-oxabicyclo[3.3.0]-7-octene: Unusual product of the soybean lipoxygenase-catalyzed oxygenation of curcumin, J. Mol. Catal. B: Enzym, 4 (1998) 219-227.

[58] M. Griesser, V. Pistis, T. Suzuki, N. Tejera, D.A. Pratt, C. Schneider, Autoxidative and cyclooxygenase-2 catalyzed transformation of the dietary chemopreventive agent curcumin, J Biol Chem, 286 (2011) 1114-1124.

[59] O.N. Gordon, P.B. Luis, H.O. Sintim, C. Schneider, Unraveling curcumin degradation: autoxidation proceeds through spiroepoxide and vinylether intermediates en route to the main bicyclopentadione, J Biol Chem, 290 (2015) 4817-4828.

[60] C.F. Chignell, P. Bilski, K.J. Reszka, A.G. Motten, R.H. Sik, T.A. Dahl, Spectral and photochemical properties of curcumin, Photochem Photobiol, 59 (1994) 295-302.

[61] T. Atsumi, K. Tonosaki, S. Fujisawa, Comparative cytotoxicity and ROS generation by curcumin and tetrahydrocurcumin following visible-light irradiation or treatment with horseradish peroxidase, Anticancer Res, 27 (2007) 363-371.

[62] T.A. Dahl, W.M. McGowan, M.A. Shand, V.S. Srinivasan, Photokilling of bacteria by the natural dye curcumin, Arch Microbiol, 151 (1989) 183-185.

[63] F. Zsila, Z. Bikadi, M. Simonyi, Circular dichroism spectroscopic studies reveal pH dependent binding of curcumin in the minor groove of natural and synthetic nucleic acids, Org Biomol Chem, 2 (2004) 2902-2910.

[64] D. Masone, C. Chanforan, Study on the interaction of artificial and natural food colorants with human serum albumin: A computational point of view, Comput Biol Chem, 56 (2015) 152-158.

[65] G.T. Sigurdson, P. Tang, M.M. Giusti, Natural Colorants: Food Colorants from Natural Sources, Annu Rev Food Sci Technol, 8 (2017) 261-280.

[66] J. Baell, M.A. Walters, Chemistry: Chemical con artists foil drug discovery, Nature, 513 (2014) 481-483.

[67] S. Winter, N. Tortik, A. Kubin, B. Krammer, K. Plaetzer, Back to the roots: photodynamic inactivation of bacteria based on water-soluble curcumin bound to polyvinylpyrrolidone as a photosensitizer, Photochem Photobiol Sci, 12 (2013) 1795-1802.

[68] F. Cieplik, A. Pummer, J. Regensburger, K.A. Hiller, A. Spath, L. Tabenski, W. Buchalla, T. Maisch, The impact of absorbed photons on antimicrobial photodynamic efficacy, Front Microbiol, 6 (2015) 706.

[69] A.B. Hegge, T.T. Nielsen, K.L. Larsen, E. Bruzell, H.H. Tonnesen, Impact of curcumin supersaturation in antibacterial photodynamic therapy--effect of cyclodextrin type and amount: studies on curcumin and curcuminoides XLV, J Pharm Sci, 101 (2012) 1524-1537.

## Highlights

- Novel curcuminoids bearing cationic substituents were prepared by different synthetic routes with good yields
- The derivatives exhibit excellent water solubility, improved photostability and low aggregation.
- Effective photokilling of *E.coli* was possible without the addition of permeabilizing agents
- Ten micromolar of the most active compound achieved a 7 $\log_{10}$ decrease of *E. coli* after light activation

## Graphical abstract